12-2019

Structure Elucidation of a Pyrrolobenzodiazepine Alkaloid and a Biologically Active Polyketide Produced by Rhodococcus sp. MTM3W5.2 via Two-Dimensional NMR Spectroscopy

Garrett Johnson
East Tennessee State University

Recommended Citation

Johnson, Garrett, "Structure Elucidation of a Pyrrolobenzodiazepine Alkaloid and a Biologically Active Polyketide Produced by Rhodococcus sp. MTM3W5.2 via Two-Dimensional NMR Spectroscopy" (2019). *Electronic Theses and Dissertations.* Paper 3681. https://dc.etsu.edu/etd/3681

Structure Elucidation of a Pyrrolobenzodiazepine Alkaloid and a Biologically Active Polyketide

Produced by *Rhodococcus* sp. MTM3W5.2 via Two-Dimensional NMR Spectroscopy

_____

A thesis

presented to

the faculty of the Department of Chemistry

East Tennessee State University

In partial fulfillment

of the requirements for the degree

Master of Science in Chemistry

_____

by

Garrett Adam Johnson

December 2019

_____

Dr. Abbas G. Shilabin, Chair

Dr. Bert C. Lampson

Dr. Ismail Kady

Keywords: Nuclear Resonance Spectroscopy, Natural product, *Rhodococcus*, polyketide

ABSTRACT

Structure Elucidation of a Pyrrolobenzodiazepine Alkaloid and a Biologically Active Polyketide

Produced by *Rhodococcus* sp. MTM3W5.2 via Two-Dimensional NMR Spectroscopy

by

Garrett Adam Johnson

As the battle against ever-increasing drug resistence bacteria rages on, novel and sometimes

more complex natural products can be used to combat this. In this study, two-dimensional NMR

techniques were utilized to collect a complete spectral data set for two natural products. The first

structure, a synthesized Pyrrolobenzodiazepine alkaloid natural product was confirmed through

these methods. The second, a strain of *Rhodococcus*, MTM3W5.2, produces a novel

antibacterial molecule in broth cultures and the active compound was fractionated using a

Sephedex LH-20 column. Chromatographic purification yielded a pure sample at 58.90 minutes,

RT.58. HRMS data deduced an exact mass of 911.5490 Da, equivalent to a molecular formula of

$C_{52}H_{78}O_{13}$. Several major spin systems were constructed from the 2D-NMR spectra. However,

due to limited sample quantity in compound with a large molecular weight and product

instability, the long range HMBC signals needed to connect these fragments have not yet been

obtained.

ACKNOWLEDGEMENTS

TABLE OF CONTENTS

5

LIST OF FIGURES

LIST OF ABBREVIATIONS

1D	One Dimensional
2D	Two Dimensional
NMR	Nuclear Magnetic Resonance
DEPT	Distortionless Enhancement by Polarization Transfer Spectroscopy
COSY	Correlations Spectroscopy
HSQC	Heteronuclear Single-Quantum Coherence Spectroscopy
HMBC	Heteronuclear Multiple-Bond Correlation Spectroscopy
ppm	Parts per million
HR-MS	High-Resolution Mass Spectroscopy
PBD	Pyrrolobenzodiazepine
MeOD	Deuterated Methanol
$CDCl_3$	Deuterated Chloroform
Da	Dalton
mL	Milliliter
g	gram
μL	Microliter
MHz	Megahertz
RT	Retention Time

CHAPTER 1

INTRODUCTION

Natural product discovery and elucidation is a growing field in the effort to develop novel antibiotics in order to combat the ever-increasing problem of drug resistent bacteria. This is just one of the many end use products that utilize the biological activity that natural products obtain. Dating back to the discovery of penicillin over 75 years ago, more than 23,000 natural product species have been identified and characterized in the fields such as pharmaceuticals, herbicides, insectacides[1]. As interest in this field has grown throughout the late 20th and early 21st centuries, so has the applied techniques to aid in this advancement.

The first 30 years of natural product discovery followed a very systematic archytype : (1) phenotypic screening, (2) compound isolation and structural characterization, (3) mode of action studies in some cases, (4) preclinical development, and if successful, (5) clinical development and commercialization. One technique in particular that has shown great effect in the second step of structural characterization is the development and implementation of Nuclear Magnetic Resonance techniques. These advanced NMR techniques have helped in not only eliminating the dereplication of known compounds quicker but also gave way to the complete structural elucidation of larger, more complex natural product species[2].

The scope of this research thesis will focus on the theory of various NMR techniques and how those can be utilized in order to validate the exact structural makeup of three differing natural product species. The first species being a Pyrrolobenzodiazepine (PBD) alkaloid analogue, being researched as a novel β-lactam antibiotic to combat the ever-increasing β-lactamase-mediated resistance.[3] These PBD analogues have also been reported to serve as anticancer therapeutics due to uniques guanine binding charateristics.[4] The second species is

most likely that of a polyketide derivative, *Rhodococcus,* MTM3W5.2, as previously reported by the research group.[5]

Chemical Shift

The basis to the theory behind NMR spectroscopy is built on the principles of nuclear spin, more importantly the nuclear spin in the presence of a magnetic field. This was first discovered in the 1950's when ^{1}H and ^{31}P nuclei were observed to absorb energy when placed into a magnetic field frequency that was specific to the nucleus itself. Once absorbed, nuclei would then resonate, with different atoms within the same molecule resonating at different frequencies. These differences in resonances are what are used to determine the chemical structure of a molecule.[6]

The spin of an electron can be denoted as the spin quantum number (m_s), this electron has both angular momentum and orbital angular momentum as it spins around a given axis. This momentum is a vector, therefore possessing both magnitude (1/2) and direction (+ or -).[7] Atomic nuclei that possess even numbers of protons and neutrons have zero spin with all other atoms said to have a non-zero spin. A given atom with non-zero spin has a magnetic moment, which can be illustrated as bar magnets in figure 1. Undisturbed, the magnet has an equal probability of any random orientation. When an external magnetic field, B_o, is applied, the magnet is forced to align with or against the magnetic field.[8]
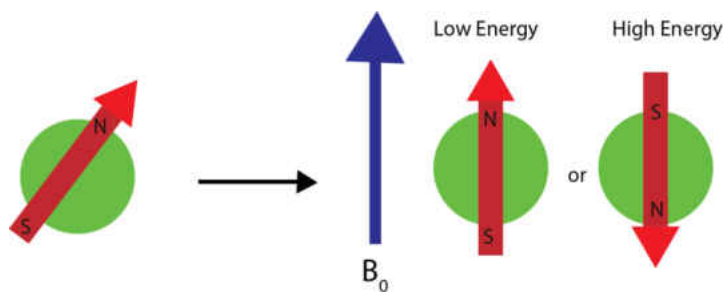
Figure 1. Magnetic Moment under an applied magnetic field[8]

The presence of electrons determines how great the effect of the external magnetic field will have on a given nucleus of a molecule. As the charged electrons orbit the nucleus a magnetic field is created and acts upon the nucleus, creating slight changes in energy levels. This phenomenon is known as shielding.[8] Inequivalent nuclei experience different magnetic fields dues to the local electronic environment, this change in energy requires a different frequency to excite the spin flip which allows for differentiation in the NMR spectrum. In figure 2, the effect of localized electrons is illustrated to describe how their magnetic field can shield the nucleus from the externally applied magnetic field.
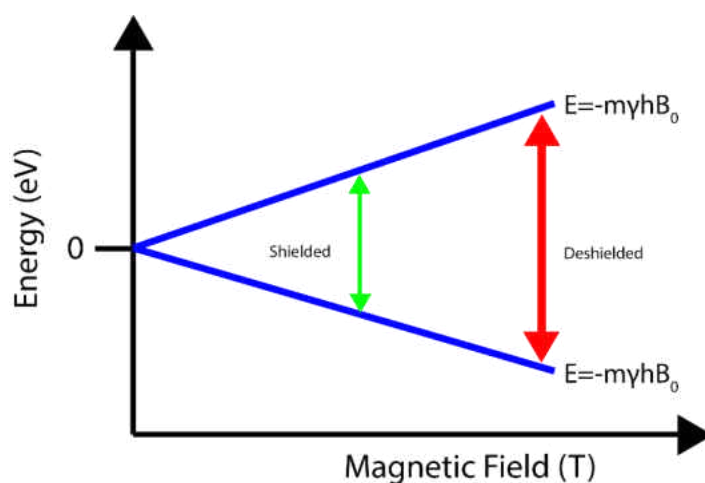
Figure 2: Shielding effect of localized electons[8]

Chemically inequivalent environments can be interpreted through the use of Fourier Transforming the NMR signal. This results in a spectrum with an arrangement of peaks that corresponds to a unique chemical environment. Figure 3 is an example of a typical ^{1}H NMR spectra for the natural product menthol, displaying numbered peaks at varying chemical shifts,

each unique to their electronic environment within the molecule.
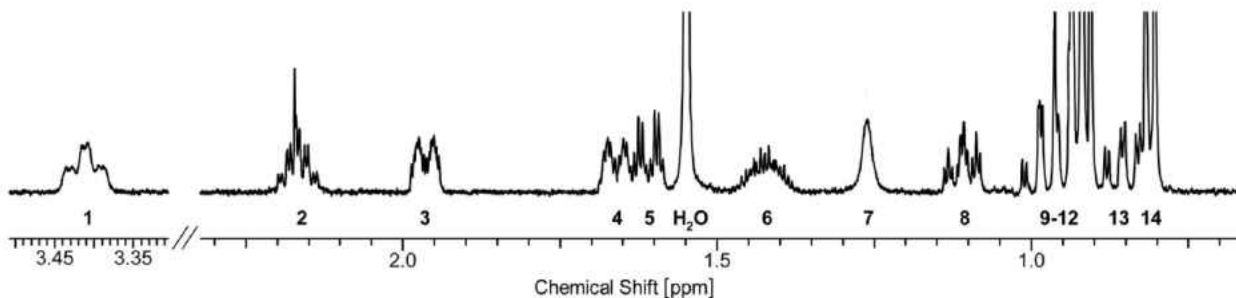
Figure 3: ^{1}H NMR of menthol[9]

The integration of area underneath each numbered peak in Figure 3 is directly proportional to the number of each given nuclei, in this case protons, within that specific environment.[8]

Sample Preparation

A high-quality NMR tube should always be used, poor quality tubes will result in poor spectra, this explains why typical NMR tubes are so expensive. A standard NMR tube is typically a cylindrical glass 5mm diameter. Smaller, more specialized NMR tubes are available in order to increase sensitivity however can be very expensive.[9]

Depending on the sample, 1-5 mg is commonly standard for an organic molecule with ^{1}H NMR, while 5-50mg is reasonable for ^{13}C NMR. Preparing an NMR tube with too little sample will hamper the signal therefore possibly giving an incomplete spectrum, while a sample with too much will cause an increase in viscosity of the sample solution leading to broad peaks.[10]

Commonly, a solvent height of 5cm is used for NMR experiments. The cylindrical tubes are inserted into a spinner which will be spun around inside of the instrument by air. A typical spinner is shown in Figure 4.
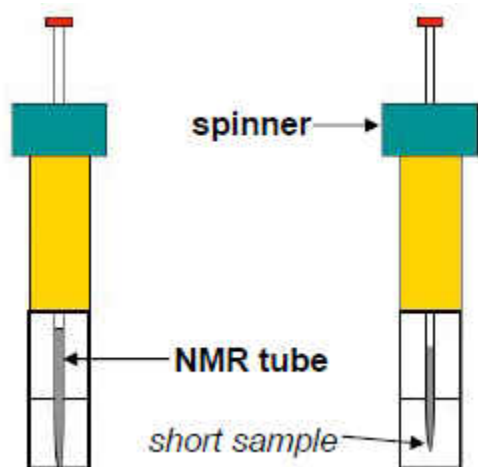
Figure 4: Typical NMR tube with spinner[11]

The vertical position of the tube in Figure 4 will be set by the depth gauge, indicated by the tube resting on the bottom of the gauge.

Distortionless Enhancement by Polarization Transfer Spectroscopy

An alternative to traditional decoupled ^{13}C-NMR experiments is a Distortionless Enhancement by Polarization Transfer (DEPT) experiment. DEPT experiments differ from the classic ^{13}C in that it is a spectral editing sequence which can be used to produce different signals based off of the type of carbon nuclei present in the molecule. Specifically, DEPT-135, uses a 135-degree decoupler pulse which in turn yields a spectrum that positively phases methyl (CH_3) and methine (CH) carbons while negatively phasing methylene (CH_2) carbons. Quaternary carbons (C) give no signal in a DEPT-135 experiment because the large one-bond heteronuclear

J-coupling is used for polarization transfer.[12] This allows for complete determination of all carbon multiplicities within a molecule.

Comparison between the standard decoupled ^{13}C spectrum and the DEPT-135 spectrum allows easy identification of quaternary carbons by looking for absent peaks in the DEPT when compared to the original ^{13}C spectrum.
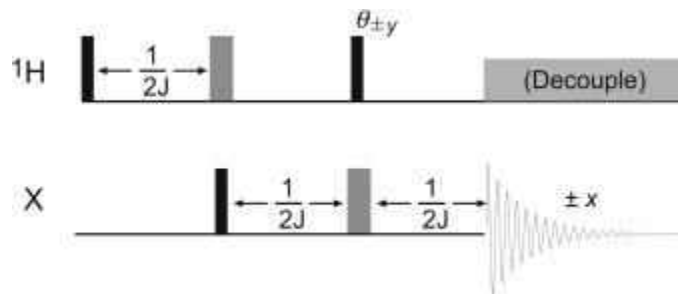
Figure 5 : Pulse sequence for a DEPT-135[13]

The DEPT sequence depicted in figure 6 begins with a 90^0 H pulse after which, under the influence of proton-carbon coupling, proton magnetization evolves. A period of 1/2J elapses, resulting in the two proton satellite vectors being anti-phase. A new 90^0 C pulse is applied in which both transverse proton and carbon magnetization evolve coherently, this is termed as multiple quantum coherence. Unlike the typical transverse magnetization that is observed in single quantum coherence NMR, multiple quantum coherence cannot be directly observed because it induces no signal in the detection coil. Thus, this signal produced must be transferred back into single quantum coherence for it to be of any use.[14]

Changing the proton decoupler pulse angle changes what multiplicity signals are detected and how they are phased. Using a 90^0 decoupler pulse produces a carbon spectrum containing only carbons with a single attached proton, methine (CH). Switching to a 45^0 decoupler pulse will produce a carbon spectrum containing only carbons with protons directly attached, all of

14

which are positively phased. Quaternary carbons are not observed. Example spectra of each

decoupled pulse angle is depicted below in figure 6 for the terpene andrographolide.
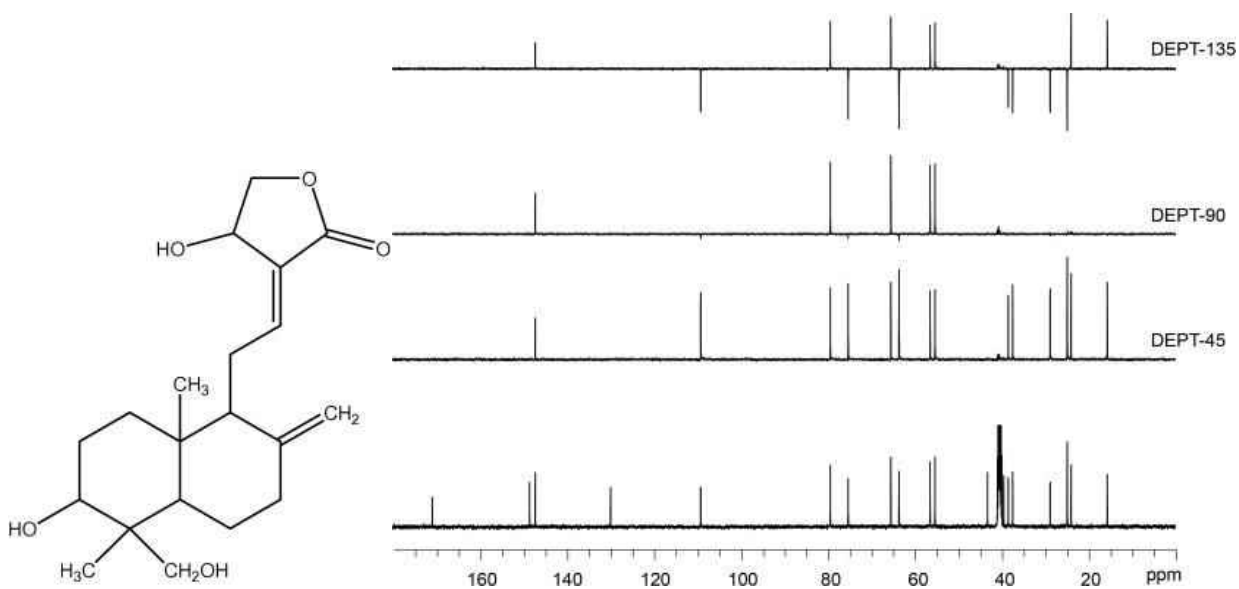
Figure 6: Andrographolide structure (left) and ^{13}C, DEPT-45, 90, and 135 spectra[15]

Homonuclear Correlation Spectroscopy

Apart from the introduction of Fourier Transfer NMR, the application of

multidimensional spectra contributed the greatest leap in NMR spectroscopy, both of which have

been acknowledge by a Nobel Prize.[16] Correlated Spectroscopy, COSY, is a useful two-

dimensional method for determining which protons are coupling with each other in a given

molecule. The pulse sequence for this two-dimensional experiment can be seen below in figure

7.
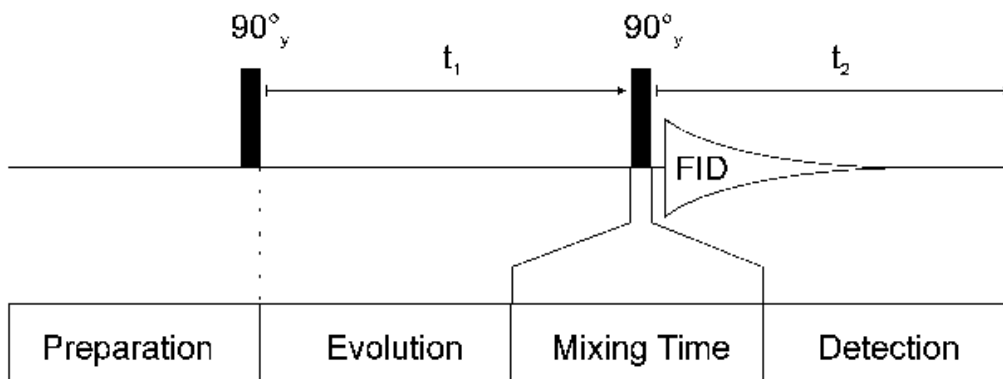
Figure 7: Pulse Sequence for a two-dimensional COSY-90 experiment[16]

Similar to the anatomy of a one-dimension NMR experiment, the two-dimensional pulse sequence also consists of a beginning preparation and finishing detection phase. A two-dimensional experiment also incorporates an indirect evolution time, t_1, and a mixing sequence. Once the nuclei are prepared the spins can begin to precess freely for any given amount of time, as determined by experimental parameters, during time t_1. As the spins are precessed the magnetization of the first nucleus is labelled, and the chemical shift is developed. This magnetization is then transferred from the first nucleus to the second nucleus during the mixing time. This magnetization transfer can be accomplished in one of two ways; scalar coupling ("through-bond") or dipolar coupling ("through-space").[17] For this instance, a COSY experiment transfers magnetization through scalar couplings. At the end of the experiment, t_2, the magnetization is labelled with the chemical shift of the second nucleus and the data is then processed for both nuclei.[16]

In the case of COSY, the spectrum is homonuclear since both evolution periods detect signals of the same ^1H isotope, therefore both axis in the COSY spectrum correspond to the

proton NMR spectrum. An example topology is depicting for a typical homonuclear ^{1}H,^{1}H-COSY spectrum below in figure 8.
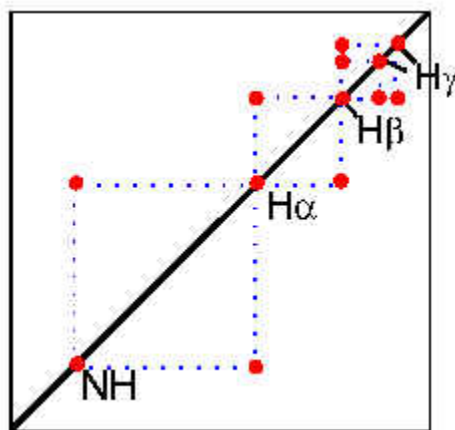
Figure 8: Example topology of ^{1}H,^{1}H-COSY spectrum[16]

A typical COSY spectrum contains two types of signals, diagonal and cross peaks. Diagonal signals can be seen in figure 8 as red peaks along the bold line running from bottom right to top left of the spectrum. This diagonal of peaks can be viewed as a plane of symmetry, dividing the spectrum into equivalent halves.

The diagonal peaks in figure 8 result from magnetization that was not changed during the mixing phases of the experiment. This is contributed from equal frequencies in both dimensions, indicating that the magnetization remained on the same nucleus throughout both evolution times, t_1 and t_2, respectively.[17]

All peak signals located off of the diagonal are referred to as cross peaks. These signals originate from nuclei that exchanged different magnetizations during the mixing phase. This is due to a difference in the frequency between the first and second nucleus in both dimensions, indicating a detectable interaction between the two nuclei. These interactions are transferred magnetizations through scalar coupling between nuclei two to three bonds apart.[17] Protons within

a molecule that lie more than three bonds apart do no give cross peak signals in the spectrum due to the fact the ^{4}J coupling constants are essentially a value of 0.[17]

There are two common types of COSY experiments, COSY-45 and COSY-90 (depicted in figure 8). These differ in the degree of the pulse angle for the second pulse, 45^0 instead of 90^0.[18] The advantage of using a COSY-45 instead of COSY-90, particularly in large molecules, is that the diagonal signals produced are less pronounced, making cross peak assignments much easier around the diagonal. So, although the COSY-90 experiment is higher in sensitivity, the COSY-45 provides a cleaner spectrum for analysis.[18] This aids in the interpretation of complex and overlapping ^{1}H spectrum.

Heteronuclear Single-Quantum Coherence

A heteronuclear single-quantum correlation, HSQC, NMR experiment is used to determine the direct, single bond correlations between nuclei of two different types within a molecule.[19] This experiment provides a contour plot of correlations between directly bonded ^{1}H and X-heteronuclear, most commonly ^{13}C and ^{15}N. A simplified outlook of HSQC experiments is to assume the combination of information given from DEPT-135 and ^{1}H spectra into a single spectrum to which each proton can be assigned to their directly bonded heteroatom. HSQC replaced the incumbent heteronuclear correlation spectroscopy, HETCOR, due to the fact that HSQC is based upon proton-detection instead of carbon-detection in HETCOR, offering higher sensitivity due to the naturally abundant ^{1}H and faster acquisition times. [20] The pulse sequence for a ^{1}H,^{13}C-HSQC is depicted in figure 9.
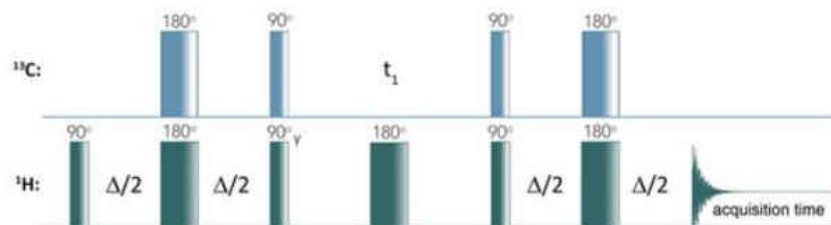
Figure 9: Pulse sequence for ^{1}H,^{13}C-HSQC[20]

Similar to the previously described COSY sequence, this two-dimensional heteronuclear pulse sequence involves the same three major parts; Preparation, Evolution, and Mixing. This particular pulse sequence utilizes the INEPT sequence during the beginning phase, as evident by the 90^0-180^0-90^0 sequence for ^{1}H and 180^0-90^0 for the ^{13}C.[20] This portion completes the preparation phase. The evolution takes place during the ^{13}C spins, during which an 180^0 pulse is applied only to the ^{1}H nucleus. The magnetization is then evolved and data are transferred back to ^{1}H nucleus where it is detected. This is how the more sensitive proton nucleus is used for detection, there in encompassing the advantage over the aforementioned HETCOR experiment.[21]

An additional spin echo can also be utilized to decouple the signal.[20] This simplifies the spectrum by collapsing multiplets down to a single peak, similar to the traditional decoupled ^{13}C experiment. This is achieved by running sequential experiments, purposefully reversing the phase of one specific pulse, this changes the sign of the undesired peaks therefore when the two spectrum are subtracted only the desired decoupled peaks are remaining in the spectrum.[22]

In the HSQC spectrum, the contour plot provides information through the use of three independent axes. On two of them, the F1and F2, the one-dimensional spectra of each heteronucleus is plotted. In the HSQC example of the sugar moiety sucrose, displayed in figure

10, the ^{1}H spectrum is plotted along the horizontal F2 axis while the ^{13}C spectrum is plotted along the vertical F1 axis.[22]
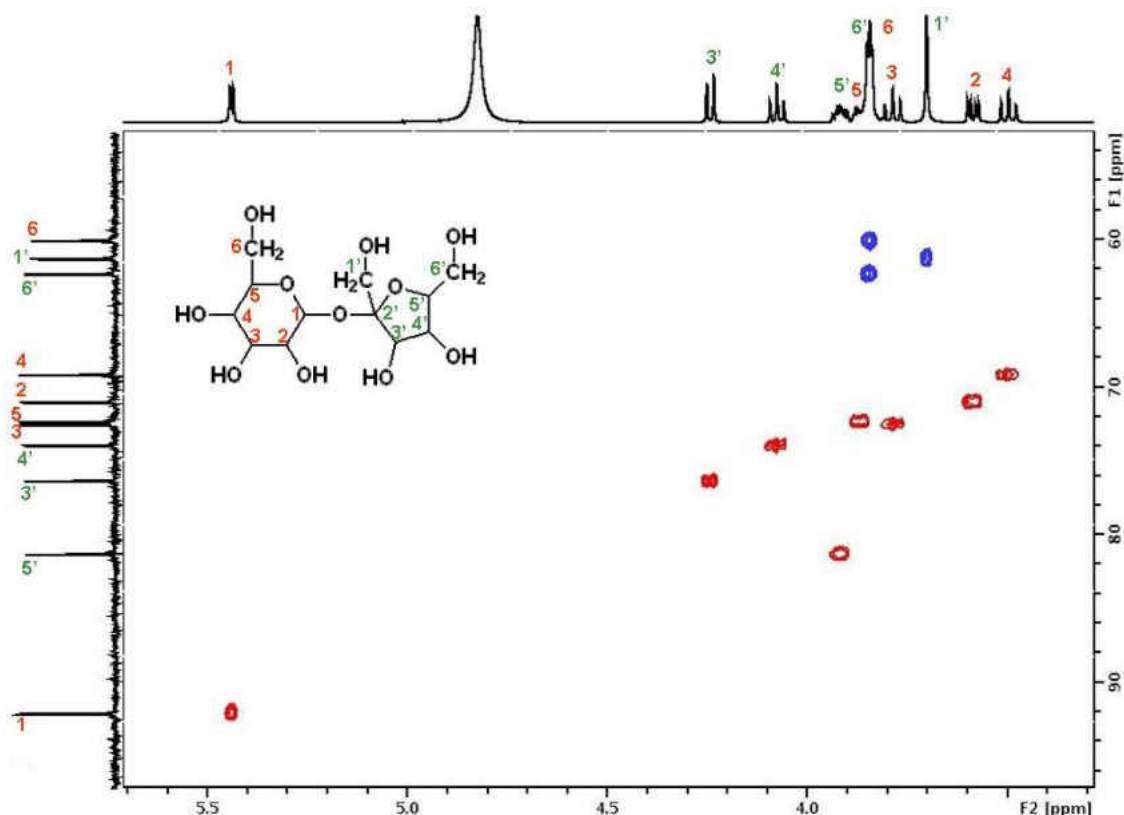
Figure 10: HSQC of sucrose[22]

The third axes is the intensity of each contour peak being phased in or out of the window plane, indicated by color. Similar to how DEPT-135 gives information regarding the multiplicity of each individual carbon through indication of being either positively or negatively phased, HSQC also quickly resolves this ambiguity. In the example of sucrose in figure 10, each methyl (CH$_3$) and methine (CH) are positively phased as indicated by a red contour peak, while each methylene (CH$_2$) are negatively phased and appear as blue contours in the given spectrum.

Heteronuclear Multiple-Bond Correlation

Heteronuclear multiple-bond correlation, specifically ^{1}H,^{13}C- HMBC, experiments give rise to the long-range correlations between protons and carbons that are most often two to three bonds away, although it is possible in some instances to observe correlations four or even five bonds away.[23] HMBC are particularly important in determining the connectivity of individual spin systems generated through COSY and HSQC experiments. Although, HMBC spectrum often tend to be the most challenging step in the complete elucidation process. The lack of cross-peak intensity is notoriously unambiguous, leading to two and three bond cross peaks displaying very weak signal, or sometimes not at all. Inherently, when a cross peak displays adequate signal, there is no simple method for distinguishing between two, three, and four bond correlations.
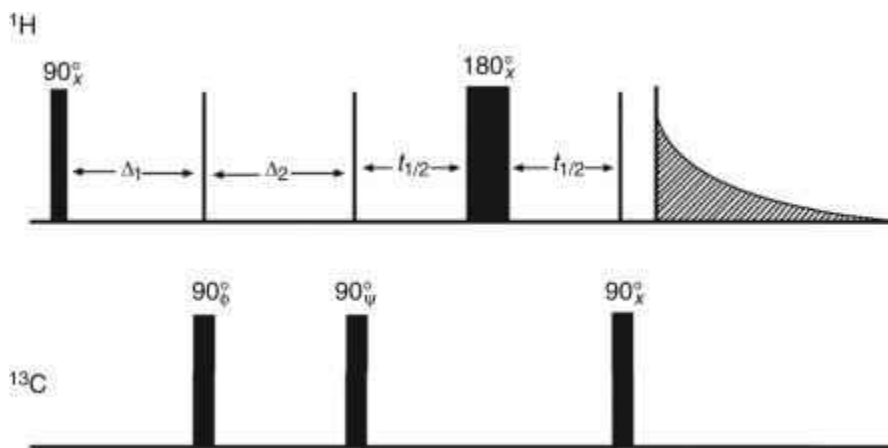
Figure 11: HMBC pulse sequence[24]

The common pulse sequence for a typical HMBC experiment can be seen above in figure 11. The first 90^0 pulse is used to eliminate the one-bond $^1J_{CH}$ correlations so that the direct connectivity cross peaks, essentially the same as recorded in HSQC spectra, are not recorded in the spectra, thus only allowing the long range ^{1}H–^{13}C connectivity to be observed. The second

90^0 pulse creates zero and double-quantum coherences, which are then interchanged during the 180^0 ^1H pulse. The final 90^0 pulse serves to modulate the ^1H signals resulting from ^1H–^{13}C multiple-quantum coherence by ^{13}C chemical shifts and homonuclear proton couplings.[25]

Standard HMBC experiments are usually optimized for long range coupling constants of intermediate size, due to this both strong and weak ^1H,^{13}C- HMBC long range couplings may result in weak cross peaks in routine HMBC. This can be addressed by acquiring two separate HMBC spectra utilizing two individual mixing delays, for example 60 and 120 ms. However, when using longer mixing delays it should be noted that the acquisitions time should also be increased to at least twice the duration of the mixing delay. This can lead to parameter sets that are considerably above the default HMBC analysis parameters in common place. [24]

Compared to standard HSQC and HMQC, a decrease in spectra intensity is often observed for the HMBC spectra. This is primarily attributed to the relatively long mixing delay (40-120 ms) in the HMBC pulse sequence, figure 11.[24] ^1H line shape of the HMBC spectra can generally be used as a predictor of adequate S/N. A narrow ^1H line width correlate with good S/N in the HMBC spectra.

In general, is not necessary to acquire a one-dimensional ^{13}C spectra if a well resolved HSQC and HMBC spectra are available for organic small molecules. However, if the species of interest possesses quaternary carbons that do not give any cross peaks in the HMBC spectra, meaning there are no protons within two to four bonds of some carbons, a typical ^{13}C spectra will need to be obtained to unambiguously distinguish between individual quaternary carbons.[26]

Unlike HSQC experiments, spectral resolution of routine HMBC in the ^{13}C-chemical shift dimension is limited. Cross peaks in the HMBC are broadened in the ^{13}C-dimension by the ^1H,^1H-coupling constants of the proton whose long-range ^1H, ^{13}C-coupling is observed. Due to

this, cross peaks belonging to carbons of very similar chemical shifts cannot be completely elucidated. It is possible to remove the interfering ^{1}H,^{1}H-coupling by using a band-selective, constant-time variant of the standard HMBC, which can produce spectra with extremely high resolution in the ^{13}C-dimension, as previously reported.[27]

Systematic Techniques for Complete Elucidation

The abilities of today's spectrophotometric instruments allow for the routine analysis of most classes of organic molecules. This is true for both complex natural products as well as synthetic creations.[28] Figure 12 highlights a few recent complete structures elucidated from various NMR techniques; platensimycin (**1**)[27], a broad spectrum nonmevalonate terpenoid antibiotic, maoecrystal V (**2**),[28] an antitumor diterpenoid, chlorofusin, a peptide-based fungal metabolite with anticancer properties, daphlongeranine B (**3**)[29], an unusual polycyclic alkaloid, and cytosporic acid (**4**)[30], a polyketide- derived HIV-1 integrase inhibitor, as well as β,β_-disilyl-substituted vinyl cations **5**[31] and cyanoresorc[5]arene **6**[32].

platensimycin (**1**)   maoecrystal V (**2**)   daphlongeranine B (**3**)

cytosporic acid (**4**)

vinyl cations (**5**)

cyanoresorc[5]arene (**6**)
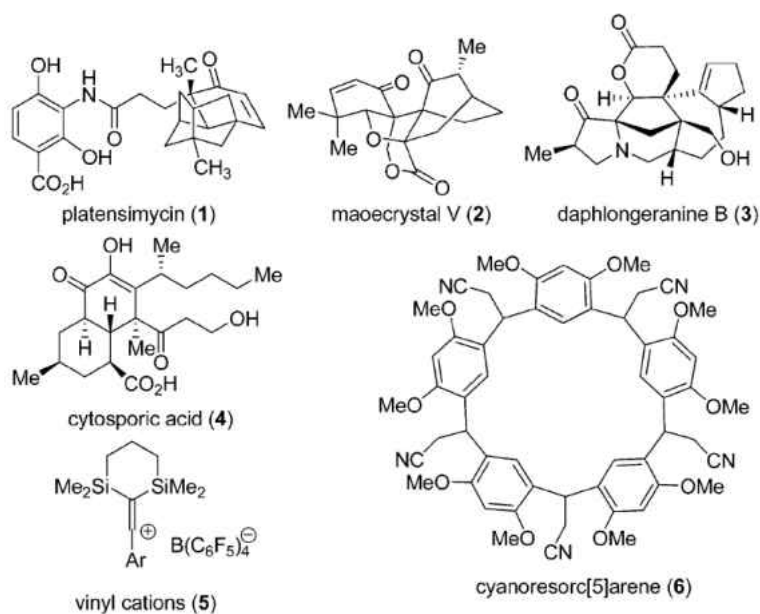
Figure 12: Recently published complete structures elucidated via NMR-spectrometric techniques[9]

For most simple, lower molecular weight organic compounds, the basic 1D 1H and 13C NMR, COSY and if needed NOESY (Nuclear Overhauser Spectroscopy) will suffice for the elucidation of complete structure.[33] It is when these basic spectra exhibit overlapping peaks or higher-order multiplet patterns which tend to complicate spectral interpretation that additional 2-dimensional experiments need to be performed. A systematic approach can be utilized to determine the degree of analysis that must be performed in order to deduce a complete structure in the most time efficient manner.[9]

Initial screening of a 1D ^{1}H and ^{13}C-NMR spectrum should reveal most of the spectral features as well as the complexity of the target species.[33] It is also worth noting that unknown overlapping peaks may be present and that experimenting with different solvents is a useful procedure to determine the best solvent based on; solubilizing effect, chemical shift, peak shape.[21] In addition, it is also prudent to obtain a molecular formula either through elemental analysis or better yet using the exact mass based off of high-resolution mass spectroscopy, HR-MS, this should be used to verify the number of protons integrated in the 1D ^{1}H-NMR spectrum matches accordingly. This will also allow the calculation of the degree of unsaturation, U, sometimes referred to as the index of hydrogen deficiency, equation 1. [34]

$$U = C + 1 - 1/2(H + X - N) \qquad (1)$$

Where C is the total number of carbons, H is the total number of hydrogens, X is the total number of heteroatoms with a valence of 1 (e.g. halides), and N is the total number of heteroatoms with a valence of 3 (e.g. nitrogen).[34] U is the total number of rings and multiple

bonds present in the molecule. Additional preliminary information can be obtained from IR or

UV/Vis spectroscopy if a specific functional group(s) is believed to be present in the species.

Next, it is most useful to identify each individual proton through HSQC experiment,

specifically if there is overlap in the 1D ^{1}H NMR spectra.[35] This will allow for the numbering of

each proton, most commonly ascending whole integers from left to right of the spectrum. In

addition, the phasing of each cross peak will give evidence to the number of protons directly

bound to a specific carbon.[35] This should eliminate the need for edited 1D ^{13}C NMR experiments

such as DEPT, which can take up excessive instrument time.[36] However, if the species contains

a large number of quaternary carbons it may be of use to compare the standard 1D ^{13}C NMR

with a DEPT experiment to more easily identify each quaternary carbon rather than comparing to

the HSQC.

After initial $^1J_{C,H}$ couplings are deduced from the HSQC it is often useful to begin

tabulating the couplings for each numbered proton. An example for the spectral data for menthol

can be seen in table 1.

Table 1: NMR Data for menthol $(CDCl_3)$[9]

ID	δ [ppm]		# of Hs	Type	Multiplet Structure		Connectivity Correlations	
	^{1}H	^{13}C			Type	Couplings [Hz]	HMBC [ppm]	COSY-45[b]
1	3.41	71.53	1	CH	td	10.4×2, 4.3	23.10, 25.82, 31.62, 45.03, 50.12	3, 8, 10
2	2.17	25.82	1	CH	sd[a]	7.1×6, 2.9	16.07, 21.00, 23.10, 50.12, 71.53	8, 11, 14
3	1.97	45.03	1	CH$_2$	dddd	12.1, 3.8×2, 2.1	22.20, 31.62, 34.51, 50.12, 71.53	1, (4), 6, 10
4	1.66	34.51	1	CH$_2$	dddd	3.4×2, 6.1, 12.4	23.10, 31.62, 45.03, 50.12, 71.53	(3), 9, 13
5	1.61	23.10	1	CH$_2$	dq	12.9, 3.3×3	31.62, 34.51, 50.12, 71.53	8, 9, 13
6	1.43	31.62	1	CH	m	(complex multiplet)	22.20, 34.51, 45.03	3, 12
7	1.35	–	1	exch.	br. s	–	–	–
8	1.11	50.12	1	CH	dddd	12.1, 10.3, 3.2×2	16.07, 45.03, 71.53	1, 2, 5
9	0.97	23.10	1	CH$_2$	m	(overlap)	34.51, 50.12	4, 5
10	0.95	45.03	1	CH$_2$	m	(overlap)	22.20, 71.53	1, 3
11	0.92	21.00	3	CH$_3$	d	7.4	16.07, 25.82, 50.12	2, (14)
12	0.91	22.20	3	CH$_3$	d	6.9	31.62, 34.51, 45.03	6
13	0.84	34.51	1	CH$_2$	dddd	12.4×2, 3.2, 1.1	(overlap)	4, 5
14	0.81	16.07	3	CH$_3$	d	7.1	21.00, 25.82, 50.12	2, (11)

Quaternary carbon atoms: none

In table 1, each unambiguous proton is numbered in column ID through use of HSQC spectrum. Each corresponding proton and carbon chemical are obtained from standard 1D ^{1}H and ^{13}C NMR (or HSQC if necessary) and reported in ppm. The chemical shift of quaternary carbons can be obtained from either the ^{13}C NMR, DEPT, or HMBC correlations. The number of hydrogens for each is determined from the integration of 1D ^{13}H NMR spectra and phase of each HSQC crosspeak.[37] The correlation data for other experiments can then be stored in additional columns. It is commonplace, to avoid bias, to record a full data set (HSQC, COSY, HMBC) before beginning spectral interpretation.[9]

Once several fragments are deduced from the HSQC and COSY spectrum, combination with HMBC data can begin to build the skeletal connectivity of the species.[38] This technique is particularly useful when transmitting through heteroatoms and quaternary carbon atoms. A tabulated list of recommended acquisition and processing parameters for each experiment can be viewed in table 2.

Table 2: Recommended acquisition and processing parameters for 2D-NMR experiments[9]

Name[a]	Comments	Situation[b]	Acquisition Parameters[c]	Calibrations[d]	Processing Parameters[e]
COSY-45 (very high)	- off-diagonal peaks indicate coupled protons - gradient-selected	short survey typical/dilute	at=0.3, d1=0.8, ni=128, 10 min at=0.3, d1=0.8, ni=256, 30 min higher resolution: ni=512, 1 h	90° (^{1}H) tune (^{1}H)	absolute-value; 2x LP in F1; sine-bell squared
HSQC (high)	- peaks are protons directly attached to carbons - phases indicate whether CH$_2$ or CH/CH$_3$ - avoid sample heating: d1 > 4at (CDCl$_3$, CD$_3$OD) d1 > 10at ([D$_6$]DMSO) - probe tuning is essential	short survey typical dilute	gradient-selected, at=0.1, d1=0.5, ni=32, j1xh=140, 30 min <500 Da: gradient-selected, at=0.2, d1=0.9, ni=128, j1xh=140, 2 h; >500 Da: gradient-selected, at=0.1, d1=0.5, ni=128, j1xh=140, 4 h - as above; use phase-cycled mode - turn spin-echo off (all peaks will have the same phase)	90° (^{1}H, ^{13}C) tune (^{1}H, ^{13}C) 90° (^{1}H, ^{13}C) tune (^{1}H, ^{13}C)	phase sensitive; 2x LP in F1; Gaussian phase sensitive; 4x LP in F1; Gaussian
HMBC (low)	- peaks are protons within three bonds of carbon - one-bond doublets are common artifacts ($J = ^1J_{C,H}$)	short survey typical dilute	- use gradient-selected mode at=0.1, d1=0.5, ni=32, j1xh=140, jnxh=8, 30 min - use gradient-selected mode <500 Da: at=0.2,d1=0.9, ni=256, j1xh=140, jnxh=8, 4 h >500 Da: at=0.1, d1=0.5, ni=256, j1xh=140, jnxh=8, 8h - use phase-cycled mode	90° (^{1}H, ^{13}C) tune (^{1}H, ^{13}C) 90° (^{1}H, ^{13}C) tune (^{1}H, ^{13}C)	absolute value; 2x LP in F1; Gaussian absolute value; 4x LP in F1; sine-bell (F1 and F2) F1 (phase), F2 (absolute); 4x LP in F1; Gaussian

CHAPTER 2

EXPERIMENTAL METHODS AND MATERIALS

NMR Solvents

Deuterated chloroform, CDCl$_3$-d (99.8% isotopic purity) +0.05% V/V TMS, was

obtained from Cambridge Isotopes Laboratories and used as is without further purification for

sample DM-002. Deuterated methyl-d$_3$ alcohol, MeOH-d$_3$ (99.96% isotopic purity) 0.75mL

ampoule was received from Aldrich Chemical Supply and was used as is without further

purification for sample RT.58.

NMR Spectroscopy Experiments

^{1}H-NMR, ^{13}C-NMR, DEPT-135, and 2D-NMR experiments including Heteronuclear Single-

quantum Correlation Spectroscopy (HSQC), Heteronuclear Multiple Bond Coherence (HMBC),

Correlation Spectroscopy (COSY) spectrum were carried out for each sample on the specific

instrument indicated below. The samples were prepared in a 5mm NMR probe unless otherwise

noted. Chemical shift values were measured in parts per million (δ, ppm). The splitting patterns

of proton signals were also designated as follows: singlet (s), doublet (d), a doublet of doublets

(dd), a doublet of the doublet of doublets (ddd), triplet (t), the quartet (q), and the multiplet (m).

DM-002

Sample was prepared and experiments performed at Eastman Chemical Company, Kingsport,

TN on a Bruker Ultraspin 500 MHz Spectrophotometer (^{1}H 600 MHz; ^{13}C 125 MHz).

Table 3. NMR Prameters for Sample DM-002

Experiment	Number of Scans	Relaxation Delay (s)
^{1}H	192	15.0
^{13}C	3500	2.00
DEPT-135	3500	2.00
^{1}H,^{1}H-COSY	16	1.48
HSQC	30	1.50
HMBC	88	1.50

RT.58

Sample was shipped and prepared at the David H. Murdock Research Institute,

Kannapolis, NC. 1D and 2D NMR experiments were performed on a Bruker Biospin II 600 MHz

spectrophotometer (^{1}H 600 MHz; ^{13}C 150 MHz).

Table 4. NMR Parameters for Sample RT.58

Experiment	Number of Scans	Relaxation Delay (s)
^{1}H	512	1.00
^{13}C	16384	2.00
DEPT-135	8192	2.00
^{1}H,^{1}H-COSY	64	1.48
HSQC	64	1.50
HMBC	128	1.50

Sample was also prepared at Eastman Chemical Company using a Wilmad Labglass 5mm

Bruker CD_3OD Shigemi tube set and 1D and 2D NMR experiments performed on a Bruker 600

MHz spectrophotometer (^{1}H 600 MHz; ^{13}C 150 MHz).

Table 5. NMR Parameters for Sample RT.58 Prepared in Shigemi Tube Set

Experiment	Number of Scans	Relaxation Delay (s)
^{1}H	1024	10
^{13}C	10,000	2.00
^{1}H,^{1}H-COSY	32	1.48
HSQC	64	1.50
HMBC	128	1.50

Spectral analysis was interpreted and completed using MestReNova x64 software.

RESULTS AND DISCUSSION

DM-002

As previously reported, the exact mass of sample DM-002 equated to 318.1481 amu. This

converts to an exact chemical formula of $C_{19}H_{18}N_4O$. Using the following formula:

Degree of unsaturation (U) = C+1-[1/2(H+X-N)]

The degree of unsaturation was determined to be 13. Analysis of the ^{1}H proton spectra

(Appendix A) integration confirmed the presence of 18 unique protons, thus agreeing with the

calculated molecular formula. The peaks in the range of 7.0 ppm and 8.2 ppm indicate the

presence of 9 aromatic protons.

Table 6. NMR Spectroscopic Data for DM-002 Sample (500MHz, CDCl₃)

ID #	δ_H, mult (J in Hz)	δ_C	carbon	COSY	HMBC
1	8.56				126.36 (**17**), 55.42(**9**)
2	8.51,s	**157.69**	CH=C		134.51(**16**), 128.11(**4**)
3	7.99	**131.39**	CH—C	7	165.90(**13**), 136.73(**15**), 132.32(**6**)
4	7.82	**128.11**	CH—C	5	157.70(**2**), 130.72(**5**)
5a, 5b, 5c	7.44, s	**130.72, 128,72**	CH=C	4	128.11(**4**)
6	7.44, t	**132.32**	CH=C	8	136.73(**15**), 131.39(**3**)
7	7.19,	**123.71**	CH=C	3, 6	126.37(**17**), 120.69(**8**)
8	7.02	**120.69**	CH=C	6	126.37 (**17**), 123.71(**7**)
9	4.40, td	**55.42**	CH—C*	11	157.47(**14**), 47.29(**10**), 26.06(**11**), 23.45(**12**)
10a, 10b	3.77	**47.29**	CH₂—C	12	55.42(**9**), 26.06(**11**), 47.29(**10**) 23.45(**12**)
11a, 11b	3.04, s, 2.17, m	**26.06**	CH₂—C	9, 12	157.47(**14**), 55.42(**9**), 47.29(**10**), 23.45(**12**)
12a, 12b	2.06, m	**23.45**	CH₂—C	10, 11	157.47(**14**), 55.42(**9**), 47.29(**10**), 26.06(**11**)
13		**165.90**	qC		

14		**157.47**	**qC**		
15		**136.73**	**qC**		
16		**134.51**	**qC**		
17		**126.37**	**qC**		

Analysis of the ^{13}C spectra, Appendix B, gave rise to a total of 17 unique carbons and identified two sets of identical carbons at 128.72ppm and 128.11ppm as indicated by the doubled peak intensity. Comparison between the ^{13}C and DEPT-135 spectra indicated the presence of five quaternary carbons due to the lack of signal in the DEPT-135. This comparison also gave rise to the presence of three methylene carbons (sp^3 -CH2-).

Analysis of the HSQC spectra (appendix E) identified each directly bonded [1]H-^{13}C, identifying ten methine (sp^2 CH) olefinic protons. Comparing the HSQC to the DEPT-135 also confirms the previously identified three methylene carbons, each of which are diastereotopic. The doublet H(10 a,b) at δ 3.77, which correlates to the multiplet H(12 a,b) at δ 2.06. H(12 a,b) in the COSY spectrum (Appendix D) then further correlates to the singlet H(11a) at δ 3.04 and multiplet H(11b) at δ 2.17. This large splitting in the chemical shift would indicate the localized presence of a stereogenic center. Proton H(9) at δ 4.40 is determined to be a sp^3 methine through comparison of the integration as well as the positive phasing in both the DEPT-135 and HSQC spectra.

In the COSY spectrum, the doublet H(3) at δ 7.99 correlates with triplet H(7) at δ 7.19. Proton H(7) further correlates to doublet H(8) at δ 7.02. HMBC spectra shows a correlation between H(3) with carbons C(13) at δ 165.90, C(15) at δ 136.73, and C(6) at δ132.32. C(15) at δ 136.73 and C(13) at δ 165.90 can both be identified as quaternary carbons when comparing the ^{13}C and DEPT-135 spectra. There are also three other identifiable quaternary carbons; C(14) at δ 157.47, C(66) at δ 134.51, and C(17) at δ 126.37, for a total of five quaternary carbons.

The overlapping of peaks of H(5) and H(6) at δ 7.45 in the ^{1}H were distinguished using the HSQC spectrum which identified three unique direct C-H linkages. Identical aromatic protons H(5a,b) at δ 7.45 are directly linked to C(5a) at δ 130.72, while aromatic proton H(5c) is bonded to C(9b) at δ 128.72. Proton H(6), also aromatic at δ 7.45, is directly bonded to C(6) at δ 132.32.

Proton H(7) correlates in the COSY to aromatic proton H(3) and (8) and further correlates in the HMBC to carbon C(17) at δ126.37 and C(8) at δ 120.69. Proton H(8) also displays a COSY correlation with H(7) and further correlations in the HMBC to carbonyl carbon C(13) at δ 165.90 and quaternary carbon C(15) at δ 136.73.

Protons H(10)-H(12) are all methylene protons, H(10) shows COSY correlation with H(12) and further correlates to carbons C(9) at δ 55.42, C(11) at δ 26.06 and C(12) at δ 23.45 in the HMBC. Proton (11a,b) are diasterotopic and correlate in the COSY to H(9) and H(12) and further correlate to carbons C(14) at δ 157.47, C(9) at δ 55.42, C(10) at δ 47.29, and C(12) at δ 23.45 in the HMBC. The final methylene H(12) correlates to protons H(10) and H(11) in the COSY and further correlates to carbons C(14) at δ 157.47, C(9) at δ 55.42, C(10) at δ 47.29 and C(11) at δ 26.06 in the HMBC. Carbons 13-17 are all quaternary carbons.
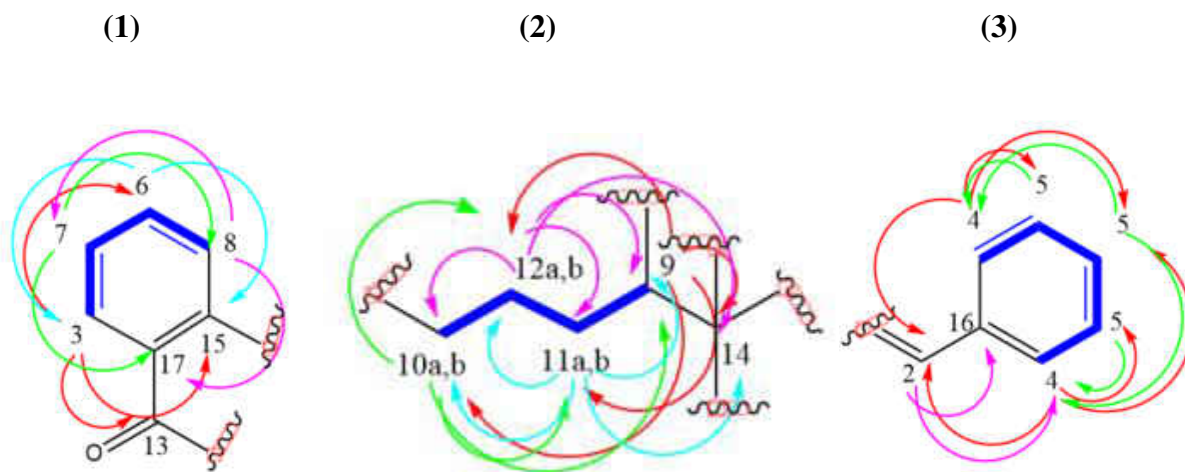
Figure 13: Structural Fragments deduced from each DM-002 spin system

Each fragment deduced from the ^{1}H,^{1}H-COSY spectra can be seen in figure 13 as bold blue connections. The spin systems created from HMBC spectra can be seen as each uniquely colored set of arrows.

When the individual spin systems are pieced together, it can be concluded that the hypothesized structure of DM-002 is supported by the spectral data collected from the 1D and 2D NMR analysis. The structure of DM-002 can be seen below in figure 14.
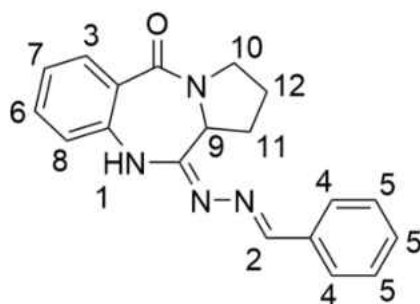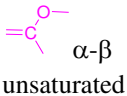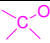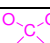

Figure 14: Confirmed structure of sample DM-002

RT.58

Once the pure *Rhodococcus sp.* **MTM3W5.2 RT.58** was obtained, a systematic

approach was taken to determine the molecular structure. Beginning with the HRMS, an exact

mass of a molecular formula of $C_{52}H_{78}O_{13}$ was determined, from this formula a degree of

unsaturation is calculated to be 14. The spectrometric data is consolidated below in table 7.

Table 7. NMR Spectroscopic Data for Sample RT.58 (600 MHz, Methanol-d_4

Proton #	δ_H, mult (J in Hz)	δ_C	Carbon	COSY (H↔H)	HMBC(H→C)
1	6.74, dd	153.66	=C, O— α-β unsaturated	5.86 (**6**), 2.49 (**25**)	167.10 (**52**), 121.52 (**6**), 80.16, 18.31 (**41**) 37.06 (**27**)
2	6.34, dd	128.67	CH=C	5.98 (**5**), 5.36 (**10**)	137.14 (**50**), 128.90 (**5**), 29.59 (**32**)
3	6.06, t	133.35	CH=C	5.42 (**8**)	132.23 (**4**), 40.60 (**30**)
4	6.03, d	131,17	CH=C	5.39 (**9**)	
5	6.00, d	128.90	CH=C	6.35 (**2**)	39.06 (**37**), 71.72 (**21**), 134.61 (**10**)
6	5.86, d	121.52	CH=C	6.72 (**1**)	167.10 (**52**) 37.06 (**27**), 18.31 (**41**)
7	5.57, dd	66.90	CH=C	1.77 (**34**)	165.93 (**52**), 61.76 (**48**), 43.78 (**25**)
8	5.47, dd	138.86	CH=C	6.05 (**3**), 2.29 (**30**)	132.38 (**3**), 131.17 (**4**)
9	5.39, dd	134.30	CH=C	6.051 (**4**)	131.17 (**4**)
10	5.35, td	134.61	CH=C	6.35 (**2**), 2.20 (**32**)	128. 36 (**5**), 70.48 (**22**), 46.19 (**32**)
11	5.24, dd	128.34	CH=C	2.29(**28**)	78.68 (**15**)
12	4.09, t	73.87	CH—O		
13	4.08, dd	78.16	CH—O		
14	4.05, d	71.36	CH—O	1.29 (**40**)	
15	3.82, d	78.68	CH—O		137.88 (**51**), 128.34 (**11**), 80.28 (**17**)
16	3.79, d	85.78	CH—O	2.39 (**27**)	71.36 (**14**), 4.89 (**44**)
17	3.69, t	80.28	CH—O		
18	3.58, t	78.86	CH—O	3.38 (**20a**)	
19	3.55, m	83.00	CH—O		18.89 (**42**), 19.13 (**43**),

20a,/20b	3.48, t / 3.41, m	73.27	CH$_2$—O	2.20 (**29**)	78.86 (**18**), 47.48(**29**)
21	3.39, d	71.72	CH$_2$—O		128.90 (**5**), 32.30 (**30**), 11.30 (**35**)
22	3.35, m	58.58	CH—C		
23	3.30, m	58.44	CH—C		
24a,/24b	2.89, m / 2.83, t	44.79	CH$_2$—C		
25	2.49, m	42.68	CH—C		98.61 (**49**), 61.76 (**48**), 66.90 (**7**)
26a,/26b	2.41, m / 2.25 m	27.79	CH$_2$—C		98.61 (**49**), 61.76 (**48**)
27	2.39, d	37.06	CH$_2$—C		
28	2.29,m	41.53	CH—C	6.75 (**1**), 3.77 (**16**), 1.12 (**41**)	121.52 (**6**), 85.78 (**16**)
29	2.20	47.48	CH—C		78.68 (**15**)
30a,/30b	2.19, m, / 1.40, s	32.30	CH$_2$—C		
31a/31b	2.10, m / 1.30, m	38.86	CH$_2$—C	138.86(**8**)	
32a,/32b	1.77, m / 1.39 m	29.59	CH$_2$—C	5.36 (**10**), 3.35(**22**), 1.41 (**34**)	58.58 (**22**)
33a/33b	1.77 dd / 1.66, m	18.90	CH$_2$—C		61.76 (**48**),
34a/34b	1.79, m /1.41, m	28.30	CH$_2$—C		61.76 (**48**), 98.62 (**49**)
35	1.71, s	11.30	CH$_3$—O		137.14 (**50**)
36a,/36b	1.71, m / 1.44 m	39.06	CH$_2$—C		
37	1.67	24.68	CH—C		128.90(**5**)
38	1.61	27.43	CH—C	1.02 (**42**), 0.94(**43**)	
39	1.60, m	42.59	CH—C	3.87 (**15**), 3.71 (**17**)	77.14 (**17**)
40	1.29, m	30.81	CH$_2$—C	0.87 (**44**), 4.05 (**14**)	
41	1.10, t	18.31	—CH$_3$	2.29 (**28**)	41.53 (**28**), 80.27 (**16**), 152.68 (**1**)
42	1.02, d	18.89	—CH$_3$	1.68 (**38**)	19.13 (**43**), 33.41 (**38**), 83.00 (**19**)
43	0.94, d	19.13	—CH$_3$	1.68 (**38**)	19.13 (**43**), 33.41 (**38**), 83.00 (**19**)
44	0.87, t	4.89	—CH$_3$	1.29 (**40**)	30.81 (**40**), 71.36 (**14**),
45	0.83, dd	17.34	—CH$_3$	2.29 (**30**)	40.64 (**30**), 71.72 (**21**), 138.86 (**8**)
46	0.49, d	13.63	—CH$_3$	1.29 (**40**)	78.68 (**15**), 80.27 (**17**), 39.09 (**40**)
47	q	53.20	>C<		
48	q	61.76	>C<O		
49	q	98.61	O>C<O		
50	q	137.15	=C<		
51	q	137.88	=C<		
52	q	165.92	O=C<O		

The ^{1}H-NMR shows a clear set of olefinic protons in the 5.25-7.0ppm range as well as seven distinct sharp methyl peaks in the upfield 0.5-1.75ppm region. The 1.5-4.0 ppm region is complicated with many overlapping and unresolved peaks, making the determination of each proton integration difficult. For this reason, the HSQC must be used to separately each unique proton signal by pairing it with its corresponding carbon atom. The ^{13}C spectra showed a total of 52 unique carbons, therefore agreeing with the molecular formula calculated from the HR-MS.
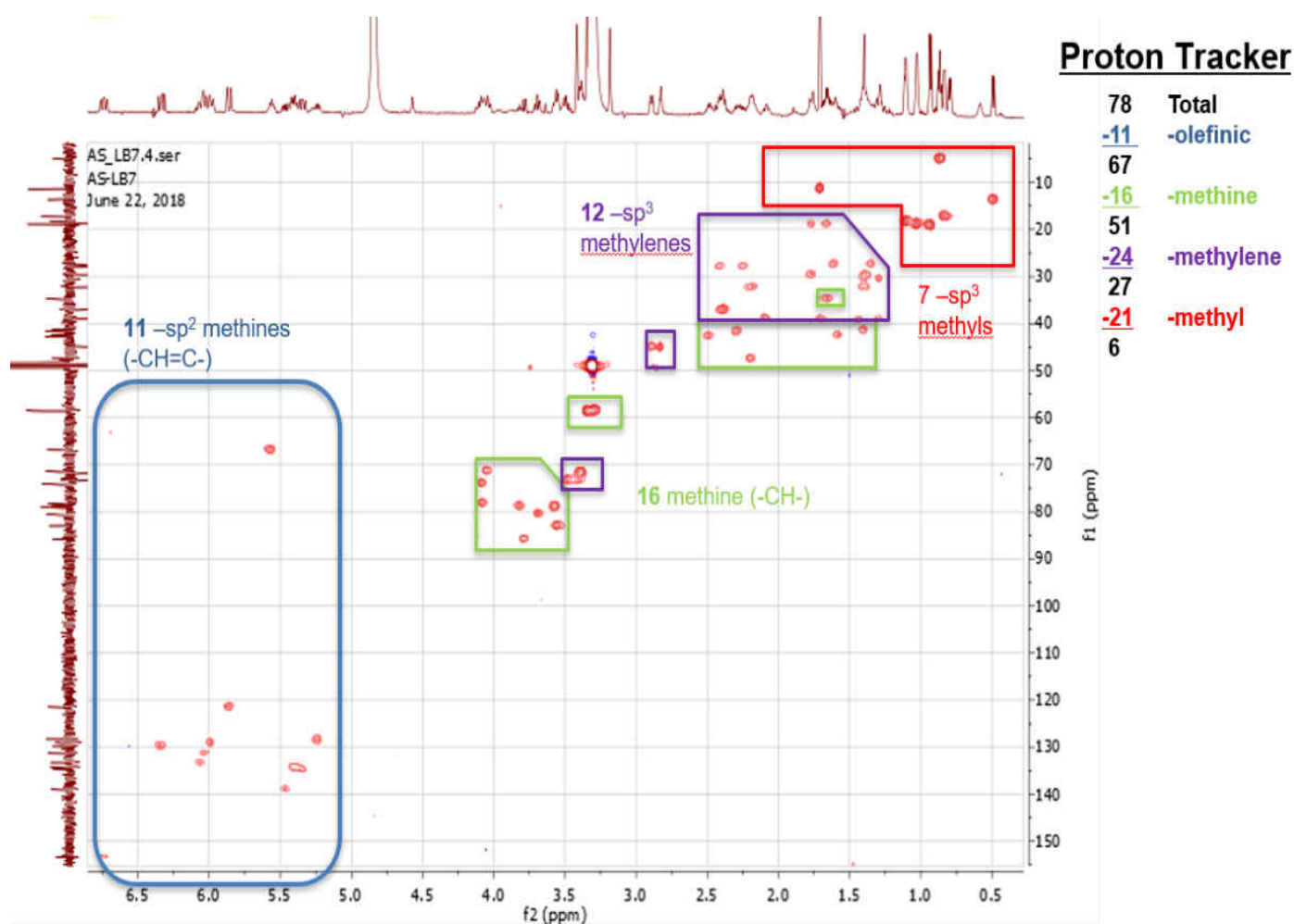
Figure 15:HSQC of RT.58 showing each proton-carbon pair as well as the hybridization of each.

These observations are confirmed by the HSQC spectra. The HSQC identifies 16 unique methine groups in the 1.25-4.20ppm region. The HSQC also gives rise to the presence of 12 sp^3 methylenes in the 1.25-3.50ppm region, this is confirmed by the negative phasing of the DEPT-135 y-axis.

A total of 72 protons can be observed in the ^{1}H and HSQC spectra. The hybridization of each proton-carbon pairing can be seen color coded in figure 15. This accounts for 11 sp^2 methines, 16 sp^3 methines, 24 sp^3 methylene protons, and 21 sp^3 methyl protons. The remaining 6 protons to be assumed as hydroxy protons within the structure, due to the exchangeability of the hydroxyl proton in the MeOD solvent.

Strong correlation between the ^{1}H, ^{1}H-COSY and HMBC also suggest that proton H(1) at δ 6.74 to be in the β-position of an α,β-unsaturated carbonyl, most likely in the form of an ester as a lactone ring, commonly associated with polyketide species.[39] Assuming a total of 13 oxygen atoms from the calculated chemical formula, removing the 6 hydroxyl oxygens as well as the 2 oxygens contributing to the lactone ring ester from the total count leaves 5 remaining oxygens to be accounted for, which can be assumed to be in the form of ether linkages.

The doublet of doublets H(1) δ 6.74 has a COSY correlation with proton H(6) δ 5.86 and with proton H(25) at δ 2.49. H(1) further correlates with carbons C(52) at δ 167.10, C(6) at δ 121.52, C(41) at δ 18.31 and C(28) at δ 41.53. Due to these correlations in the HMBC of H(1) to C(52) at δ 167.10 and that C(52) is a quaternary carbon with a chemical shift typical of a carbonyl ester, it is believed that C(1) is the carbonyl carbon of the lactone ring.

The doublet of doublets of proton H(2) at δ 6.34 has COSY correlations with protons (H5) and H(10) at δ 5.98 and 5.36, respectively. H(2) also correlates with quaternary carbon C(50) at δ 137.15, C(5) at δ 128.90, and C(32) at δ 29.59 in the HMBC. The doublet proton H(5)

also correlates with carbons C(37) at δ 24.68, C(21) at δ 71.72 and C(10) at δ 134.61 in the HMBC. H(10) further correlates with proton H(32) at δ 2.20 in the COSY. H(32) at δ 2.20 then further correlates with protons H(22) at δ 3.35 and H(34b) at δ 1.41 in the COSY as well as with carbon C(22) at δ 58.58 in the HMBC. Proton H(34b) further correlates in the HMBC with quaternary carbons C(48) at δ 61.76 and C(49) at δ 98.62.

Triplet proton H(3) has a COSY correlation with proton H(8) at δ 138.86. H(8) at δ 138.86 then further COSY correlates with proton H(30) at δ 2.29. Proton H(3) also shows a correlation with carbons C(4) at δ132.23 and C(30) at δ 32.30 in the HMBC.

The doublet proton H(4) shows a COSY correlation with H(9) at δ 5.39, this correlation is confirmed by the cross peak of H(9) with H(4) in the COSY as well as with the HMBC cross peak of H(9) with carbon C(4) at δ131.17. No further correlations are detected for proton H(4) or H(9) in the COSY or HMBC.

The doublet of doublets H(7) at δ 5.57 shows a COSY correlation with proton H(34) at δ 1.77. H(7) then further correlates with quaternary carbon C(52) at δ 165.92, C(27) at δ 37.06 and C(41) at δ 18.31.

Proton H(11) at δ 5.24 correlates in the COSY with H(28) at δ 2.29. H(11) then shows further correlation with carbon C(15) at δ 78.68.

Protons H(12) at δ 4.09, H(13) at 4.08, and H(17) at δ 3.69 do not show any correlations in the COSY or HMBC spectrums. Proton H(14) at δ 4.05 shows a COSY correlation with proton H(40) at δ 1.29. H(40) then shows further COSY correlation with proton H(44) at δ 0.87. This correlation is also reflected in the HMBC of proton H(44) with carbons C(40) at 30.81 and C(14) at δ 71.36.

Proton H(15) at δ 3.82 shows no correlations in the COSY but does show HMBC

correlations with quaternary carbon C(51) at δ 137.88, C(11) at δ 128.34 and C(17) at δ 80.28.

Proton H(16) at δ 3.79 displays a COSY correlation with proton H(28) at 2.29. H(16)

then further correlates with carbons C(14) at δ 71.36, and methyl carbon C(44) at δ 4.89.

Proton H(18) at δ 3.58 shows a COSY correlation with diastereotopic proton H(20a) at

3.48.

Proton H(19) does not show any COSY correlations but does show HMBC correlations

with carbons C(42) at δ 18.89 and C(43) at δ 19.13.

Proton H(20) shows COSY cross peak with proton H(29) at δ 2.20 and further correlates

with carbons C(18) at δ 78.86 and C(29) at δ 47.48. Proton H(29) shows further HMBC

correlations with C(15) at δ 78.68 in the HMBC.

Proton H(21) at δ 3.39 does not show any COSY correlations but does display HMBC

correlations with carbons C(5) at δ 128.90, C(30) at δ 32.30 and C(35) at δ 11.30.

Protons H(22) at δ 3.35, H(23) at 2.30, H(24) at δ 2.89 and H(27) at 2.39 do not show

any correlations within the COSY or HMBC spectrums.

Protons H(25) at δ 2.49 and H(26a,b) at δ 2.41 and 2.25 do not show any COSY

correlations however both show HMBC correlations with quaternary carbons C(49) at 98.61 and

C(48) at 61.76, in addition to H(25) also showing HMBC correlation to carbon C(7) at δ 66.90.

Proton H(28) at δ 2.29, in addition to the COSY correlations to H(1) at δ 6.75 and H(16)

at δ3.77 also shows COSY correlation to proton H(41). H(28) also displays HMBC correlations

to carbons C(6) at δ 121.52 and C(16) at δ 85.78.

Protons H(30a,b) at δ 2.19 and 1.40, respectively, H(36ab) at δ1.71 and δ 1.44 do not

show any COSY or HMBC correlations

Protons H(33a,b) at δ 1.77 and 1.66 along with H(34a,b) at δ 1.79 and 1.41 do not show

any COSY correlations but do both show HMBC correlations with carbon C(48) at δ 61.76,

along with H(34ab) also showing HMBC cross peak with carbon C(49) at δ 98.61.

Proton H(38) at 1.61 shows COSY correlations to two sets of methyl protons, H(42) at δ

1.02 and H(43) at δ 0.94.

Protons H(41)-H(46) are all sp^3 methyls, with H(41) showing COSY correlation to H(28)

at δ 2.29 and HMBC correlations to carbons C(28) at δ 41.53, C(16) at δ 80.27, and C(1) at δ

153.66. H(42) and H(43) show identical COSY and HMBC correlations with both COSY to

proton H(38) at 2.29 and HMBC to carbons C(38) at δ 33.41, C(43) at δ 19.13 and C(19) at δ

83.00. H(44) shows a COSY cross peak with proton H(40) at δ 1.29 and HMBC cross peaks with

carbons C(40) at δ 30.81 and C(14) at δ 71.36. H(45) displays a COSY with H(30) at δ 2.19 and

HMBC cross peaks with C(30) at δ 40.64, C(21) at δ 71.72 and C(8) at C(8) at δ 138.86. H(46)

displays a COSY cross peak with H(40) at 1.29 and HMBC cross peak with C(15) at δ 78.68,

C(17) at δ 80.28, and C(40) at δ 30.81.

The combination of each spin fragment into a spin system begins to piece together the

molecular structure of RT.58. A few possible structural fragments are displayed below in figure

16. Each color represents a spin system developed from each COSY correlation and each arrow

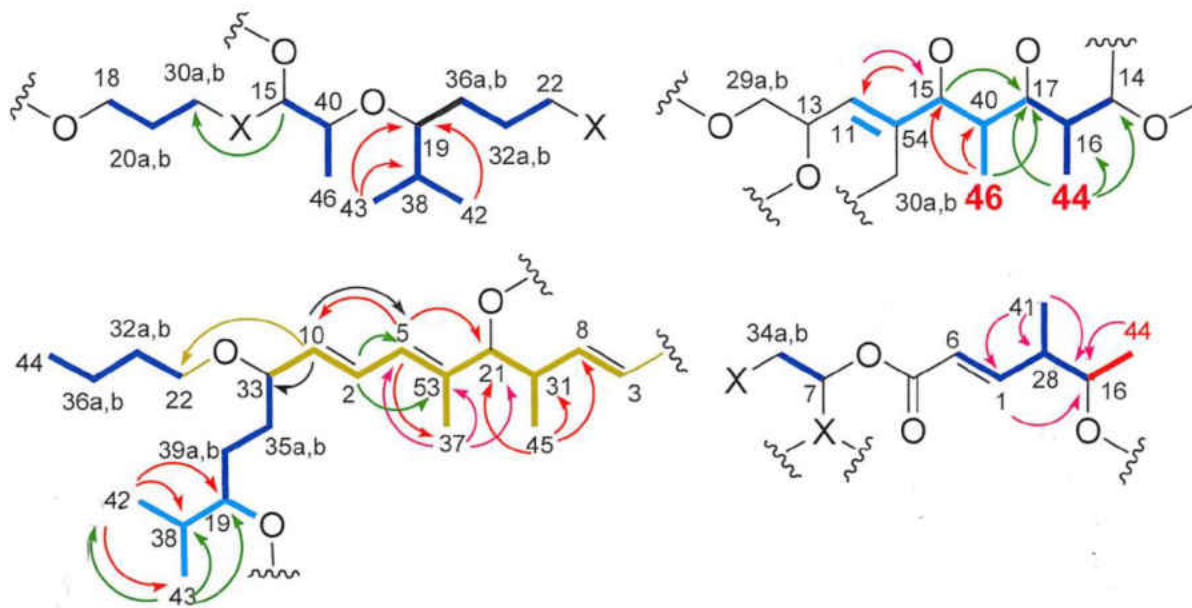represents a long-range HMBC correlation.

Figure 16:Possible partial spin systems for RT.58

Although the HMBC gives insight into neighboring identities of each unique proton, it is not sufficient to give complete evidence of a full structure. This is due to the very low sample concentration of the NMR sample itself in MeOD, this concentration is limited due to the low amount of purified RT.58 sample available. This limited sample quantity in combination with the instability of large molecular weight natural products make elucidation of a complete structure for RT.58 extremely difficult. It is theorized that the stability of larger molecular weight natural products is extremely volatile in comparison to lower molecular weight natural products, especially when taking into consideration the many trials of the purification process that must take place to provide an adequately clean natural product species.[40]

Attempts were made to improve signal strength by increase the number of scans of the HMBC analysis however, due in context to the inherently low sensitivity of the HMBC experiment itself, no improvement were observed in the quality of long-range signals needed to fully elucidate RT.58.

Another technique is to use a different NMR tube that is highly specific to both low sample concentrations and solvent effects. A Shigemi tube was obtained and the sample was reanalyzed on a 600 MHz spectrophotometer. The workings of a Shigemi tube can be seen below in figure 17.
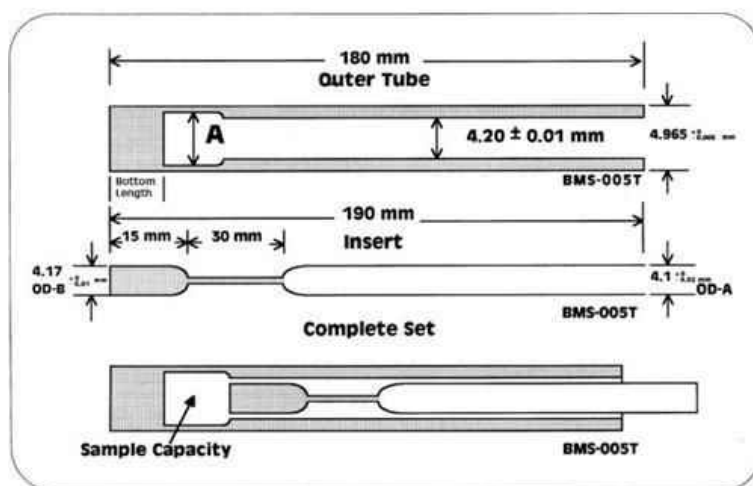
Figure 17 :Typical Shigemi tube apparatus

Shigemi tubes are specific for the type of instrument (e.g. Bruker, Varian) as well as for the solvent that the sample will be dissolved in. The typical NMR tube requires approximately 0.5-0.75 mL total volume to assure proper sample height when inserted into the instrument.[41]

A shigemi tube provides a bottom length of the specific solvent in a pure layer on the bottom of an outer tube, the sample is then dissolved and transferred into the tube. An inner tube, sometimes referred to as a plunger, that has a top layer of pure solvent is then inserted into the outer tube, forming a complete air tight seal with the middle layer of dissolved sample.[42] This provides a more concentrated sample at the proper coil height when placed into the instrument.

Unfortunately, when RT.58 was reanalyzed using a Shigemi tube, no improvements were observed in the signal strength of the long range HMBC signals. This could be due in part to the loss of sample during transitions between tubes as well as the instability effect of the natural product itself.

CHAPTER 4

CONCLUSIONS AND FUTURE WORK

Conclusions

The identity of the synthesized natural product DM-002, a Pyrrolobenzodiazepine (PBD) alkaloid was confirmed to be the desired structure through the use of 1D and 2D NMR techniques. The integration of ^{1}H NMR spectrum exactly matched the predicted number of protons as calculated by the molecular formula, provided by HR-MS. Each proton was uniquely identified using HSQC and each hybridization of carbon determined. The use of HMBC long range correlations made possible the connections of each spin fragment by providing correlations to quaternary carbon and heteroatoms. The complete structure of DM-002 is confirmed to be that of which is depicted in figure 13.

In the case of RT.58, many partial spin systems were developed and confirmed through the use of 2D NMR analysis. The main evidence of which being an alpha-beta unsaturated ester, most likely of which in the form of a macro-lactone, common for various polyketide synthase derivatives. It was determined that there were no aromatic protons or carbons in the structure. Due to the complicated and overlapping of the ^{1}H the use of HSQC was needed to uniquely identify each proton, which successfully identified 72 unique protons. The combination of ^{13}C and HSQC data confirmed the presence of 52 carbon atoms, confirming the molecular formula predicted from HR-MS to be correct. From this, it could be deduced that the remaining 6 protons must come from a hydroxy (-OH) functional group on the basis that these are exchangeable in the MeOD solvent and that no amine (-NH$_x$) functional groups were identified in the mass spectroscopy.

Through analysis of the HSQC the hybridization of each carbon atom was determined and identified with the species containing; seven sp^3 methyl groups (-CH$_3$), eleven sp^2 methines (-CH=C-), sixteen sp^3 methines (-CH-C-), and twelve sp^3 methylenes (-CH$_2$-C) eight of which are diastereotopic.

The HMBC provided information needed for the connectivity of spin fragments through the correlation of quaternary or heteroatoms, however, the long-range correlations that are needed to connect every fragment were not obtained for two reasons: i.) limited purified sample quantity led to an inadequate sample concentration in the NMR sample. ii.) the high molecular weight of 911.5490 [M+H] $^+$ of the natural product leads to an unstable product thus affecting the spectral signals and intensity overtime.

The use of a specialized Shigemi NMR tube in hopes to improve sample concentration proved to be ineffective in providing higher signal strength in the HMBC spectrum. Increased scans and longer analysis times also proved to be ineffective in providing an increase in the long-range signals needed for complete elucidation.

Future Work

More work is needed in order to provide an adequate sample for complete structural elucidation:

i.) Continued efforts around the extraction, isolation, and purification processes could provide more purified RT.58 sample which in turn could increase sample concentration of a future complete spectral analysis.

ii.) Complete 1D and 2D spectral analysis at an external facility at higher resolution (e.g. 700 or 800 MHz NMR spectrophotometer instrument) could yield higher resolution and signal strength in the poorly sensitive HMBC experiment to provide longer range couplings needed for elucidation.

iii.) Studies around the stability of the purified RT.58 could lead to advances in the storage and handling of the final product in order to prolong the desired species to be used for spectral analysis.

iv.) Studies focusing on the growth and isolation of RT.58 crystals could lead to the ability to analyze via X-ray crystallography in order to provide an absolute configuration of the species. If this effort is successful, a retrosynthetic pathway could then be analyzed and proposed as a novel route to obtaining purified RT.58 sample. This could in turn lead to an alternative means other than isolation and purification of a meniscal amount of naturally available material.

REFERENCES

1. Bérdy, J. Thoughts and facts about antibiotics: where we are now and where we are heading. *J Antibiot*. **2012**. *65,*385–395

2. Nicolaou, K. C., Snyder, Scott. Chasing Molecules That Were Never There: Misassigned Natural Products and the Role of Chemical Synthesis in Modern Structure Elucidation. *Angewandte Chemie*. **2005**. *44,* 1012-1044.

3. Annor-Gyamfi, J. K.; Jarrett, J. M.; Osazee, J. O.; Bialonska, D.; Whitted, C.; Palau, V. E.; Shilabin, A. G. Synthesis and Biological Activity of Fused Tetracyclic Pyrrolo[2,1-C] [1,4]Benzodiazepines. *Heliyon*. **2018**, *4*, 1-19.

4. Cipolla, L. Araújo, A.C. Airoldi, C. Bini, D. Pyrrolo[2,1-c][1,4]benzodiazepine as a scaffold for the design and synthesis of anti-tumour drugs. *Anticancer Agents Med Chem*. **2009**, *1*, 1-31.

5. Ward, L. Amber. Identification of Genes Required to Synthesize an Antibiotic-like Compound from the Soil Bacterium Rhodococcus sp. MTM3W5.2. M.S thesis, 2015.

6. Lambert, Joseph B and Eugene P Mazzola. Nuclear Magnetic Resonance Spectroscopy: An Introduction to Princliples, Applications, and Experimental Methods: Upper Saddle River: Pearson Education. **2004**, 6-32.

7. Housecroft, Catherine E., and Alan G. Sharpe. *Inorganic Chemistry*. 3rd ed. Harlow: Pearson Education, **2008**, *15*, 432-464.

8. Atta-ur-Rahman. Nuclear Magnetic Resonance. New York: Springer-Verlag, **1986**, *4*, 144-148.

9. Kwan, E.; Huang, S.G. Structural Elucidation with NMR Spectroscopy: Practical Strategies for Organic Chemists. *Eur. J. Org. Chem.* **2008**, 2671–2688.

10. Keeler, J. Understanding NMR Spectroscopy (2nd Ed.) Wiley, **2010**, 4-5.

11. Data Acquisition and Processing:

    https://ekwan.github.io/pdfs/nmr/lecture%205.pdf (accessed 11/17/2019)

12. Jacobsen, N. E. NMR Spectroscopy Explained: Simplified Theory, Applications and

    Examples for Organic Chemistry and Structural Biology. John Wiley & Sons, Inc. **2007,**

    360-374.

13. Breitmaier, E. Structure Elucidation by NMR in Organic Chemistry: A Practical Guide.

    3rd Revision edition. New York: John Wiley & Sons, Inc. **2002**, 215-222.

14. DEPT:

    http://science.widener.edu/svb/nmr/isobutanol/experiments.html (accessed 8/26/2019)

15. Claridge, T. High-Resolution NMR Techniques in Organic Chemistry (Third Edition).

    Elsevier Science. **2016,** 171-202.

16. Two Dimensional NMR Spectroscopy:

    http://www.cryst.bbk.ac.uk/PPS2/projects/schirra/html/2dnmr.htm (accessed 8/27/2019)

17. J. B. Lambert, E. P. Mazzola. Nuclear Magnetic Resonance Spectroscopy: An

    Introduction to Principles, Applications, and Experimental Methods, Inc. Pearson

    Education Upper Saddle River, New Jersey, **2004**, 68-72.

18. Nakanishi, Koji, ed.. One-dimensional and two-dimensional NMR Spectra by Modern

    Pulse Techniques. Mill Valley, California: University Science Books. **1990,** 138-140.

19. Keeler, James. .Understanding NMR Spectroscopy (2nd ed.). Wiley. **2010**. *209-215.*

20. Riegel, S. D.; Leskowitz, G. M. Benchtop NMR spectrometers in academic teaching.

    TrAC, **2016,** *83,* 27-38.

21. W. E. Hull. Two Dimensional NMR Spectroscopy: Applications for Chemists and Biochemists. 2nd ed. VCH, New York, **1994**, 302.

22. Columbia University-HSQC

    http://www.columbia.edu/cu/chemistry/groups/nmr/hsqc.html (accessed 8/27/209)

23. Edison, Arthur; Schroeder, Frank C.; NMR – Small Molecules and Analysis of Complex Mixtures. Comprehensive Natural Products II. *Acc. Chem. Res.* **2010,** *2,* 169-196.

24. Reynolds, W.F.; Natural Product Structure Elucidation by NMR Spectroscopy. *Pharmacognosy*. **2017**, *29*, 567-596.

25. Atta-ur-Rahman, Muhammad Iqbal Choudhar. Importany 2D-NMR Experiments: Solving Problems with NMR Spectroscopy. **1996**, 213-343.

26. D. Neuhaus; M. P. Williamson, The Nuclear Overhauser Effect in Structural and Conformational Analysis, 2nd ed. Wiley:New York, **2000**, 35-45.

27. T. D. Claridge; I. Perez-Victoria, Org. Biomol. Chem. **2003**, *1*, 3632–3634.

28. Singh, S. B. Jayasuriya, H.. Ondeyka, J. G Herath, K. B. Zhang, C. Zink, D. L.. Tsou, N. N R. Ball, G. Basilio, A.O. Geneneral Structural Elucidation with NMR Spectroscopy. *J. Am. Chem. Soc.* **2006**, *128*, 11916–11920.

29. Li, S.H. Wang, J. Niu, X.M. Y.H. Shen, H.J. Zhang, H.D. Sun, M.L. Li, Q.E Tian, Y. Lu, P. Cao, Q.T. Spectroscopic Properties of Inorganic and Organometallic Compounds Zheng, *Org. Lett.* **2004**, *6*, 4327–4330.

30. C.-S. Li, Y.-T. Di, H.-P. He, S. Gao, Y.-H. Wang, Y. Lu, J.-L. Zhong, X.-J. Hao, *Org. Lett.* **2007**, *9*, 2509–2512.

31. Jayasuriya, H. Guan, Z. Polishook, J. D. Dombrowski, A. W. Felock, P. J. Hazuda, D. J. Singh, S. B. *J. Nat. Prod.* **2003**, *66*, 551–553.

32. D'Acquarica, I. Nevola, L. Monache, G. D. Gács-Baitz, E. Massera, C. Ugozzoli, F.G. Zappia, B. Botta, *Eur. J. Org. Chem.* **2006**, 3652–3660.

33. Lambert, J. B. Mazzola E. P. Nuclear Magnetic Resonance Spectroscopy: An Introduction to Principles, Applications, and Experimental Methods, Inc. Pearson Education Upper Saddle River, New Jersey, **2004**, 363-364.

34. M. Badertscher, K. Bischofberger, M. E. Munk, E. Pretsch, A novel formalism to characterize the degree of unsaturation of organic molecules. *J. Chem. Inf. Comput. Sci.* **2001**, *41*, 889–893.

35. Claridge T. D. W. High-Resolution NMR Techniques in Organic Chemistry. *Tetrahedron*. **1999,** *19*, 117–118.

36. Bendall, M. R. Dodrell, D. M. Pegg, D. T. Polarization transfer pulse sequences for two-dimensional NMR by heisenberg vector analysis. *J. Am. Chem. Soc*. **1981**, *103*, 4603–4605.

37. Stott, K. Keeler, J. Van, Q. N. Shaka, A. J. One-Dimensional NOE Experiments Using Pulsed Field Gradients. *J. Magn. Reson*. **1997**, *125*, 302–304.

38. Bax, A. Summers, M. F. 1H and 13C Assignments from Sensitivity-Enhanced Detection of Heteronuclear Multiple-Bond Connectivity by 2D Multiple Quantum NMR. *J. Am. Chem. Soc*. **1986**, *108*, 2093–2094.

39. Shen, Ben. Polyketide biosynthesis beyond the type I, II and III polyketide synthase paradigms. *Chemical Biology*. **2003**, *7*, 285–295.

40. Staunton, J. Weissman, K. J. Polyketide biosynthesis: a millennium review. *Nat Prod Rep*. **2001**, *18*, 380-416.

41. Iowa State Univeristy-NMR sample preparation

https://www.cif.iastate.edu/nmr/nmr-tutorials/sample-preparation (accessed 9/1/2019)

42. University of Buffalo-NMR sample preparation

http://www.nmr2.buffalo.edu/nesg.wiki/NMR_Sample_Preparation (accessed 9/1/2019)

APPENDICES

Appendix A: ^{1}H spectra of DM-002
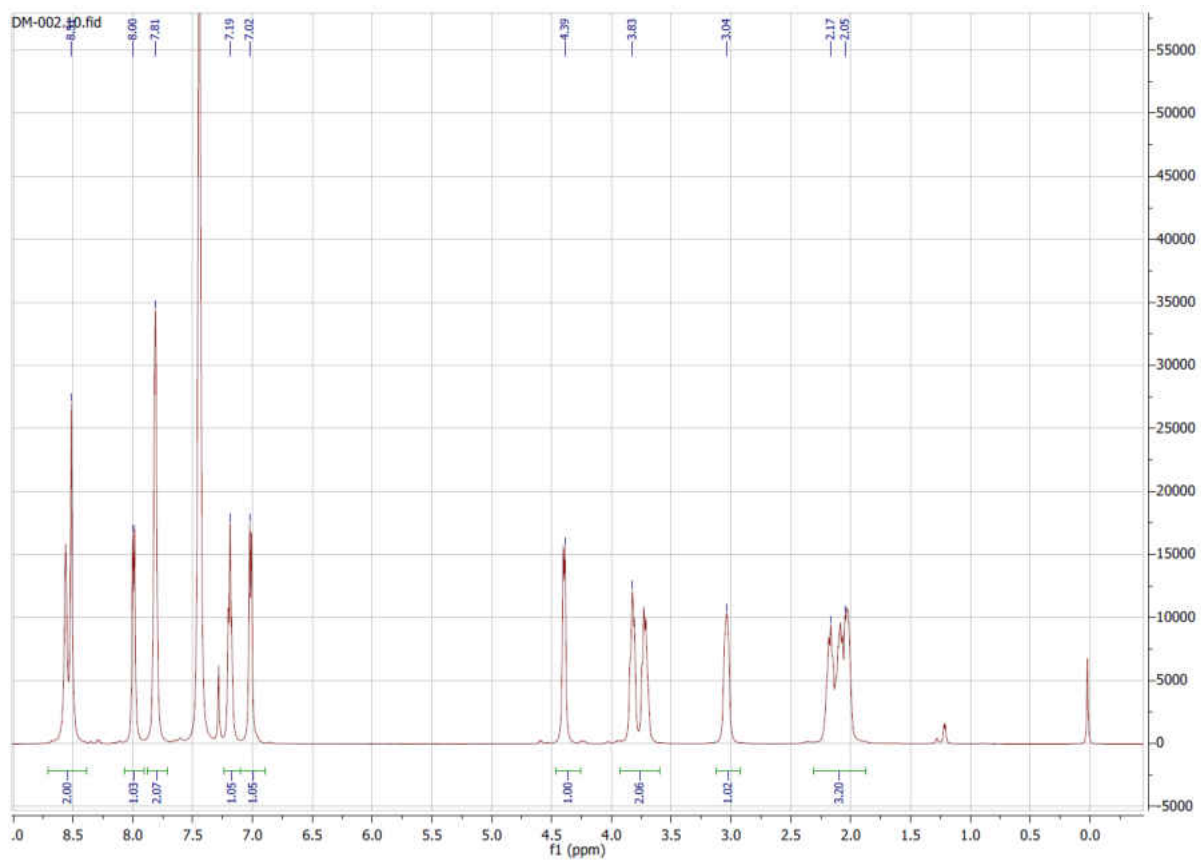
AS_LB7.3.ser
AS-LB7
June 22, 2018
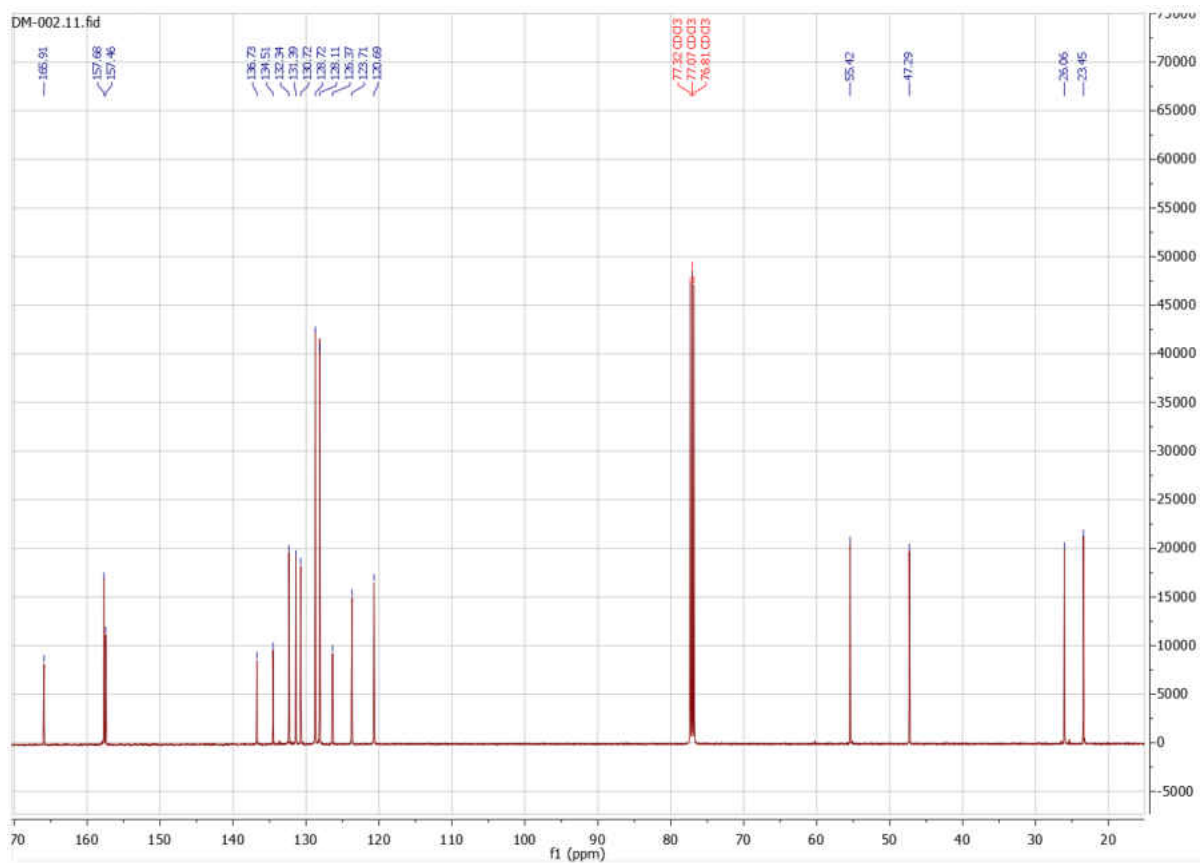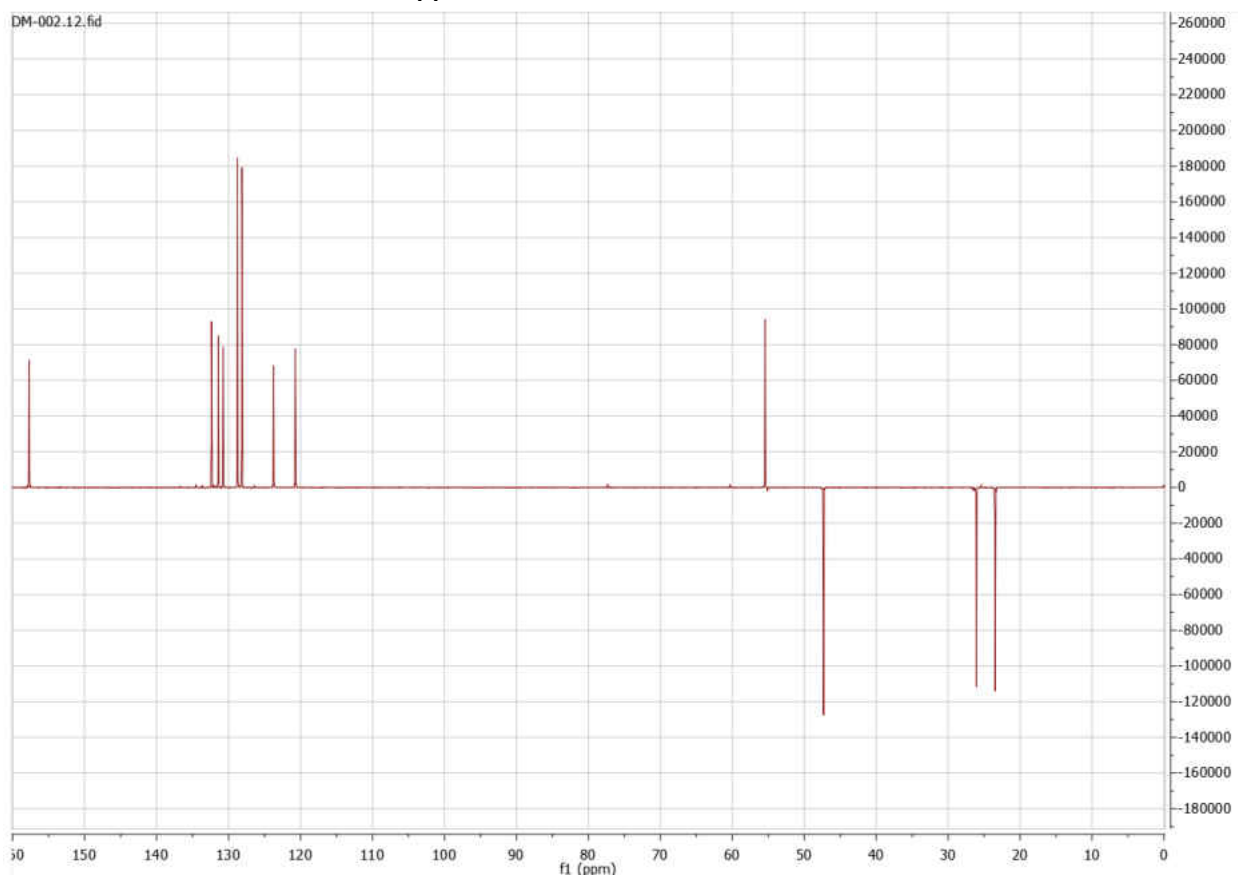
AS_LB7.4.ser
AS-LB7
June 22, 2018
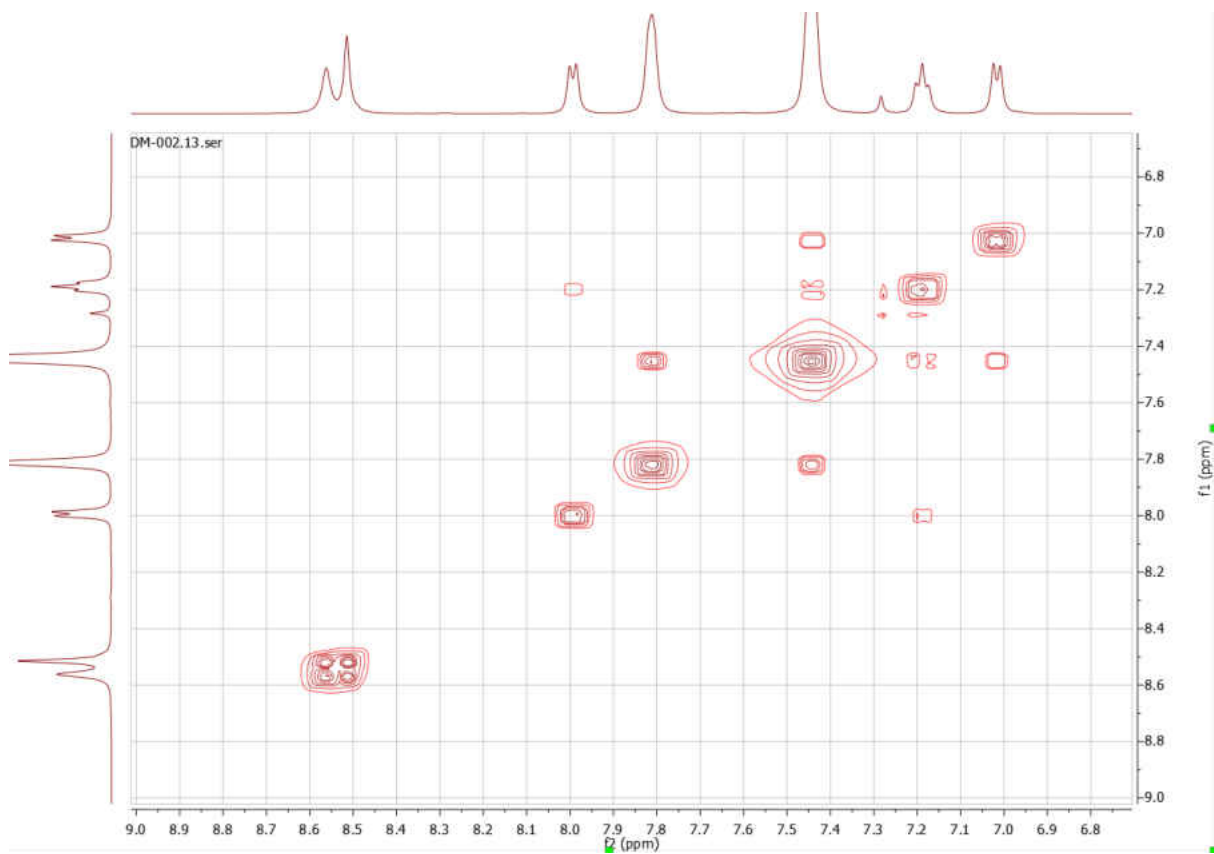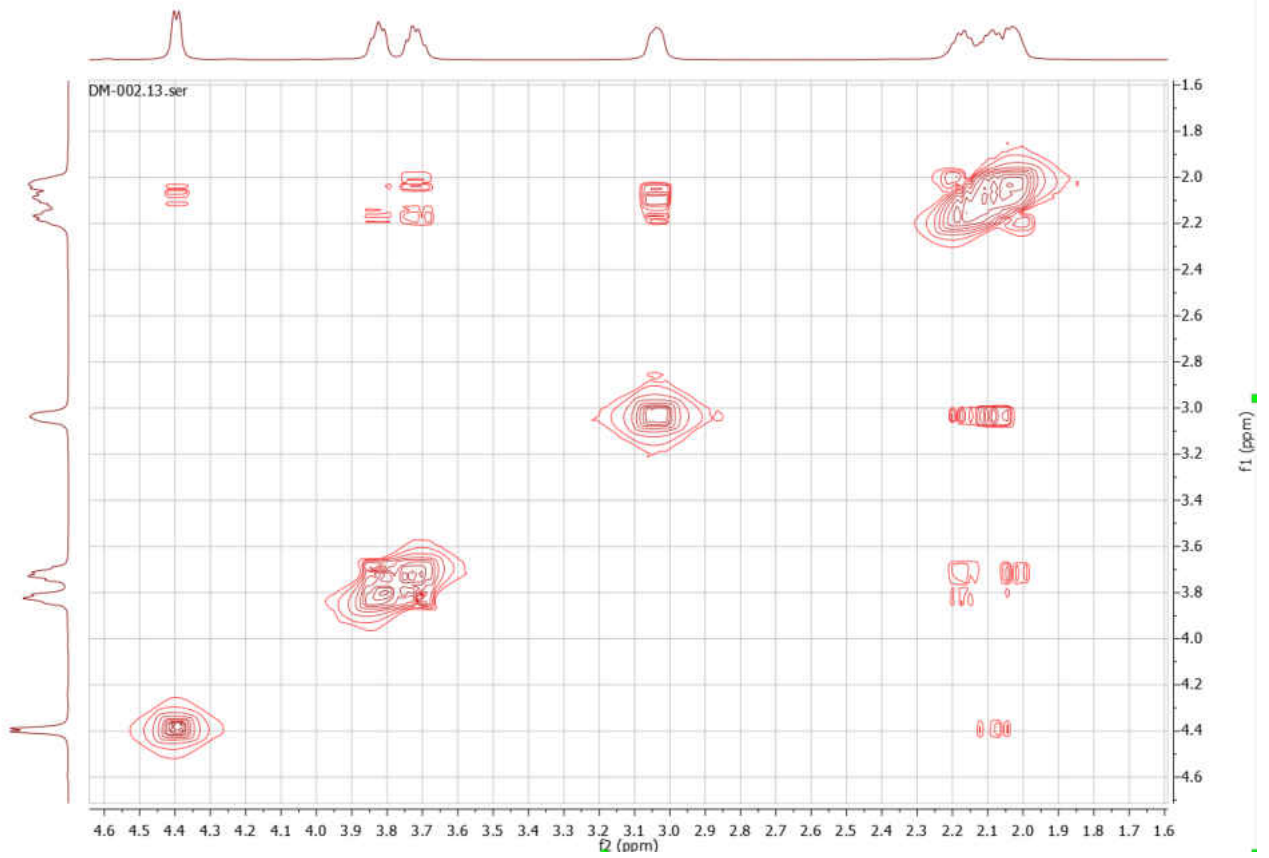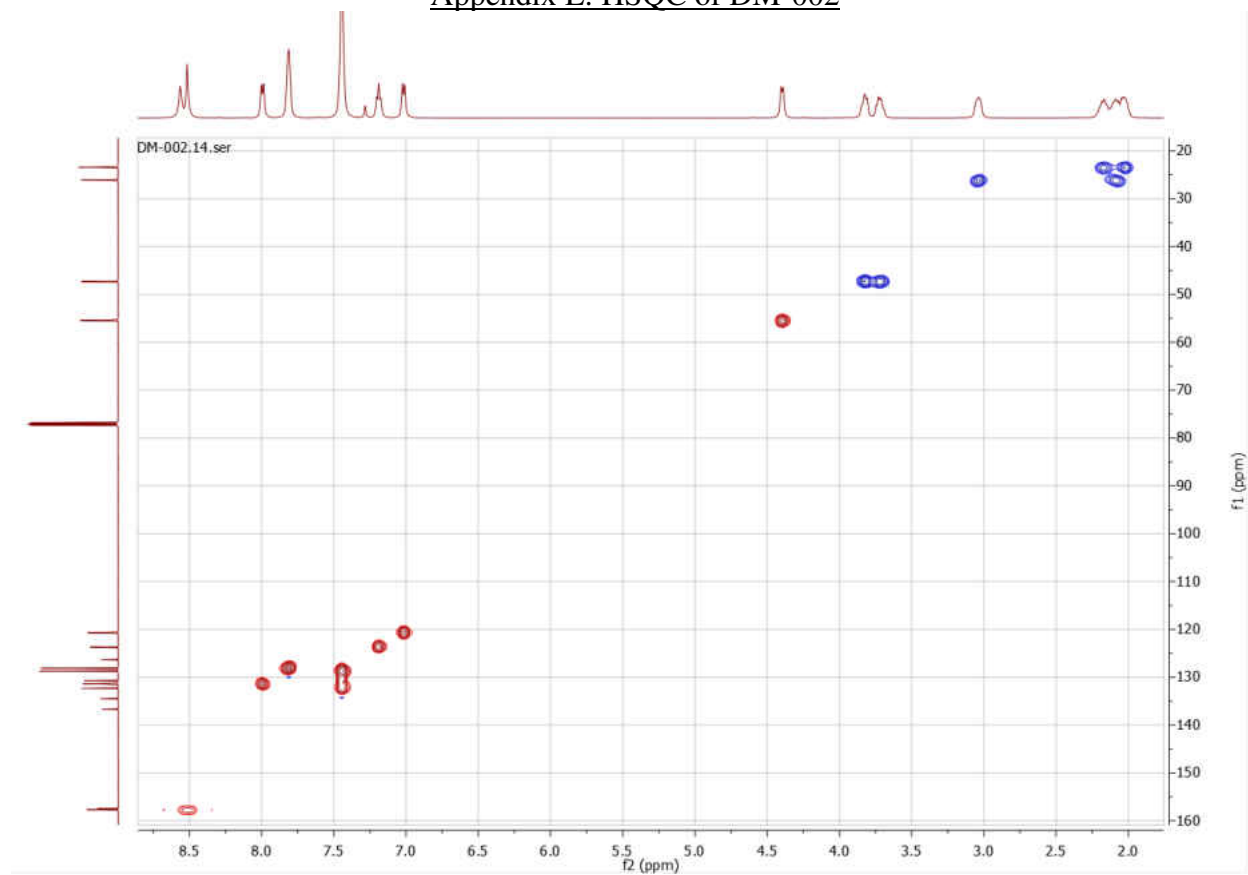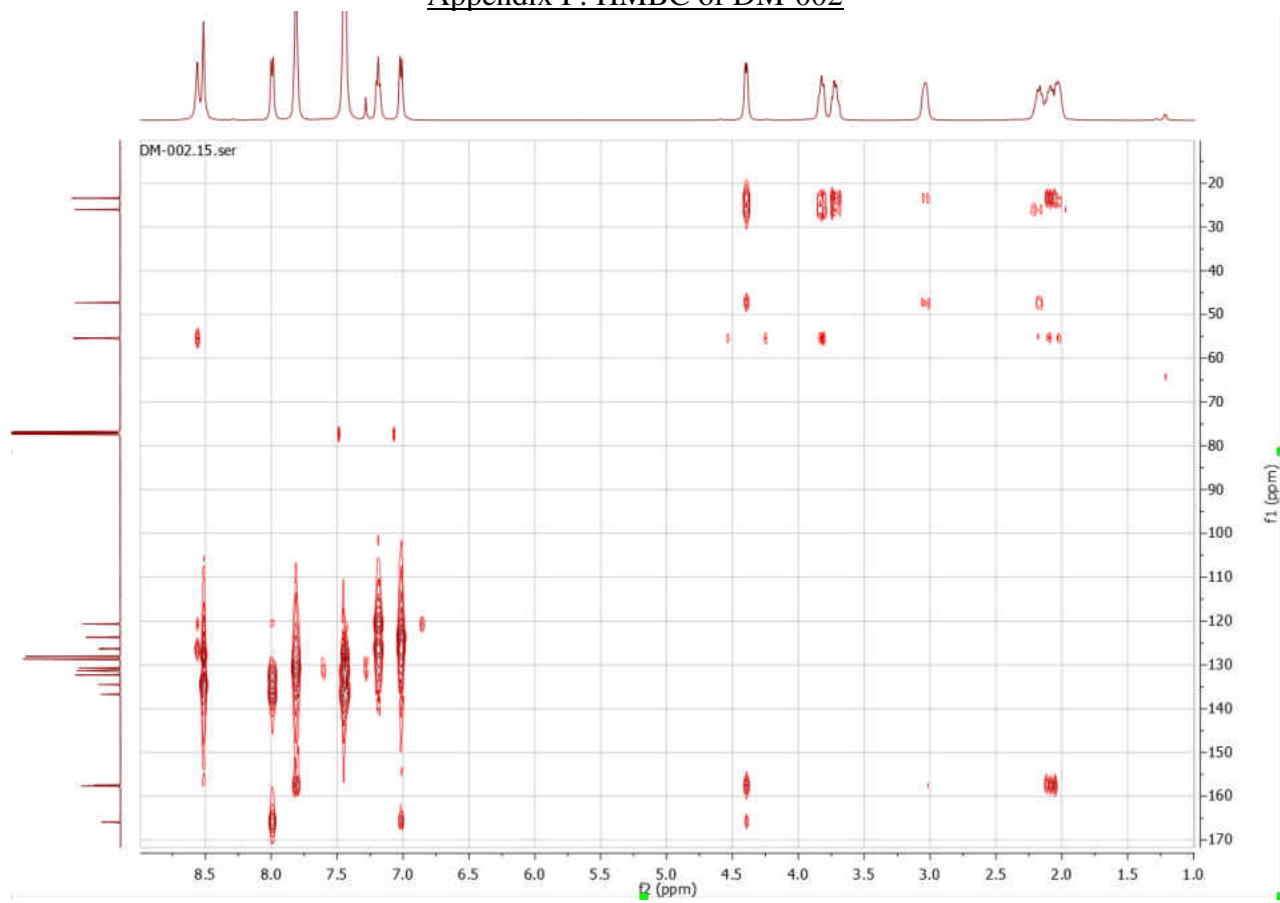
Appendix M: ^{1}H Spectrum of RT.58 Shigemi

LB-7 MeOD Shigemi tube.10.fid
Proton
D1=10s
NS=1024
Time = 3:45
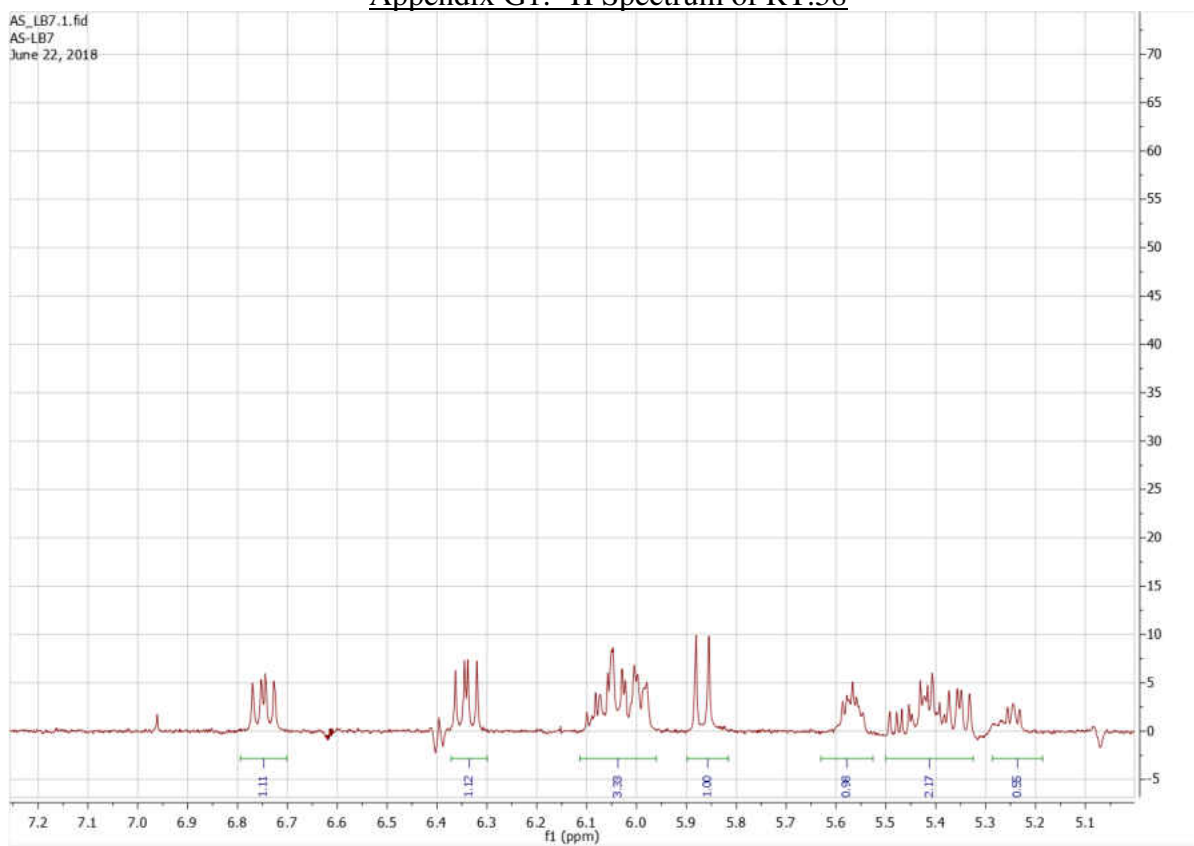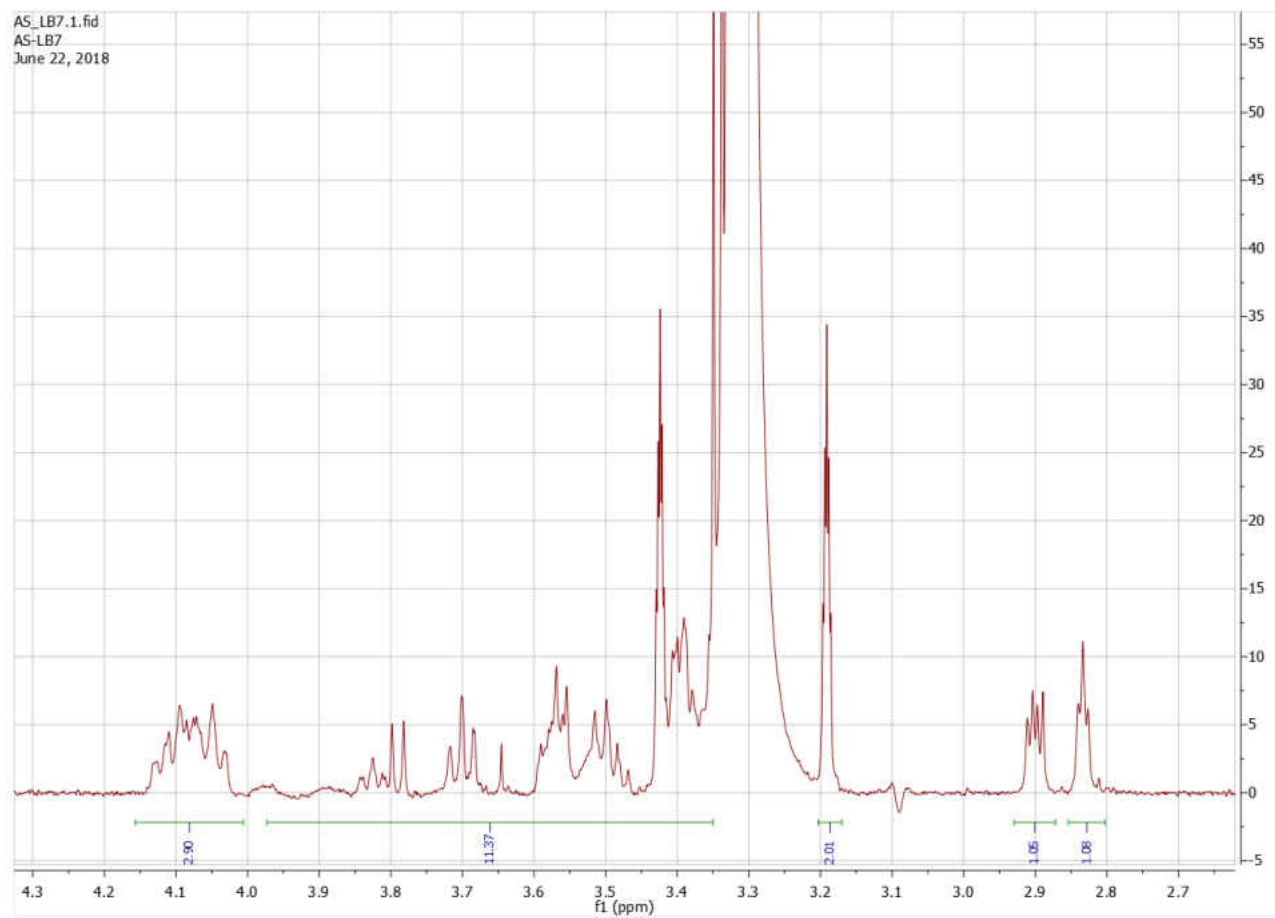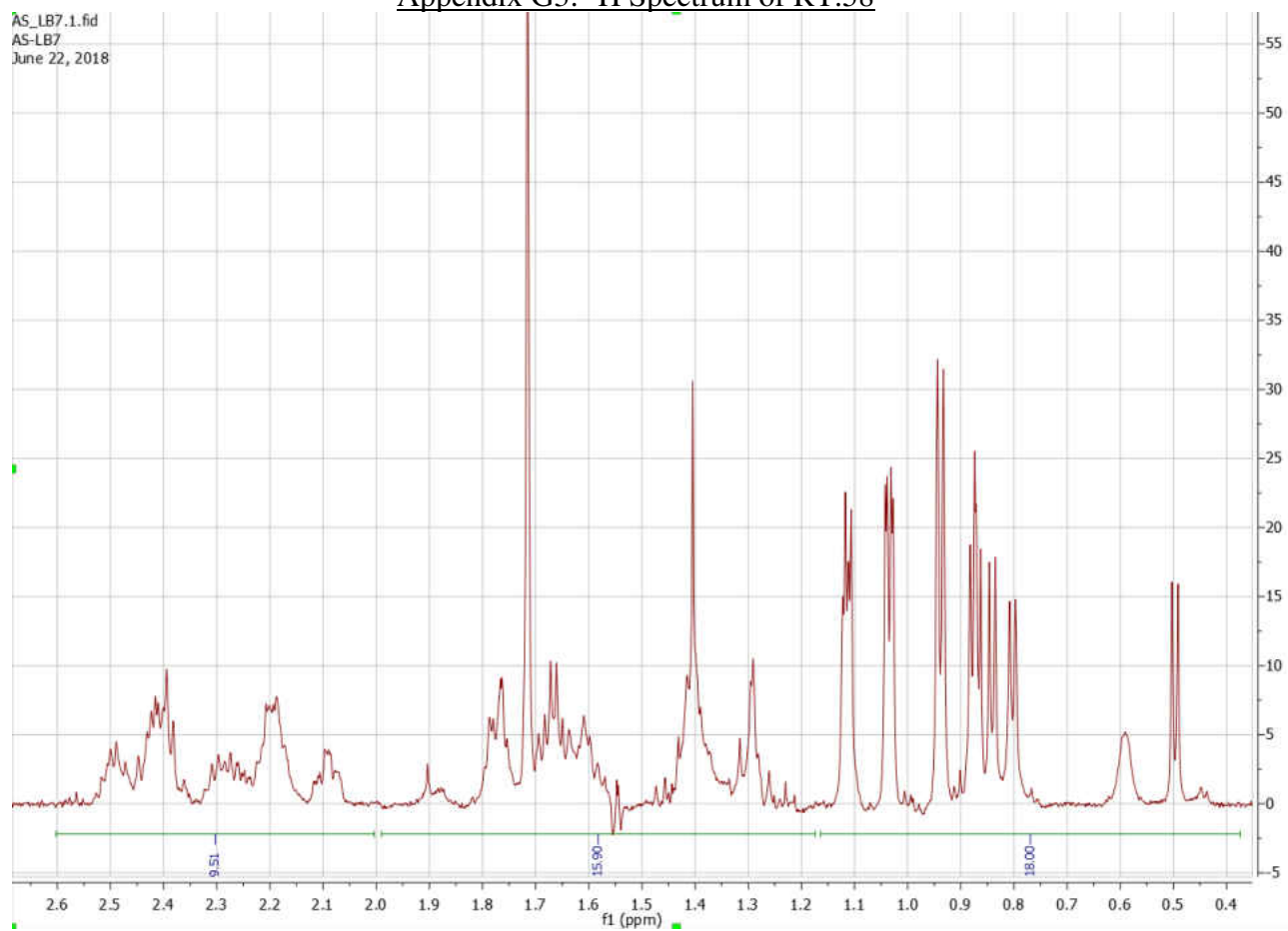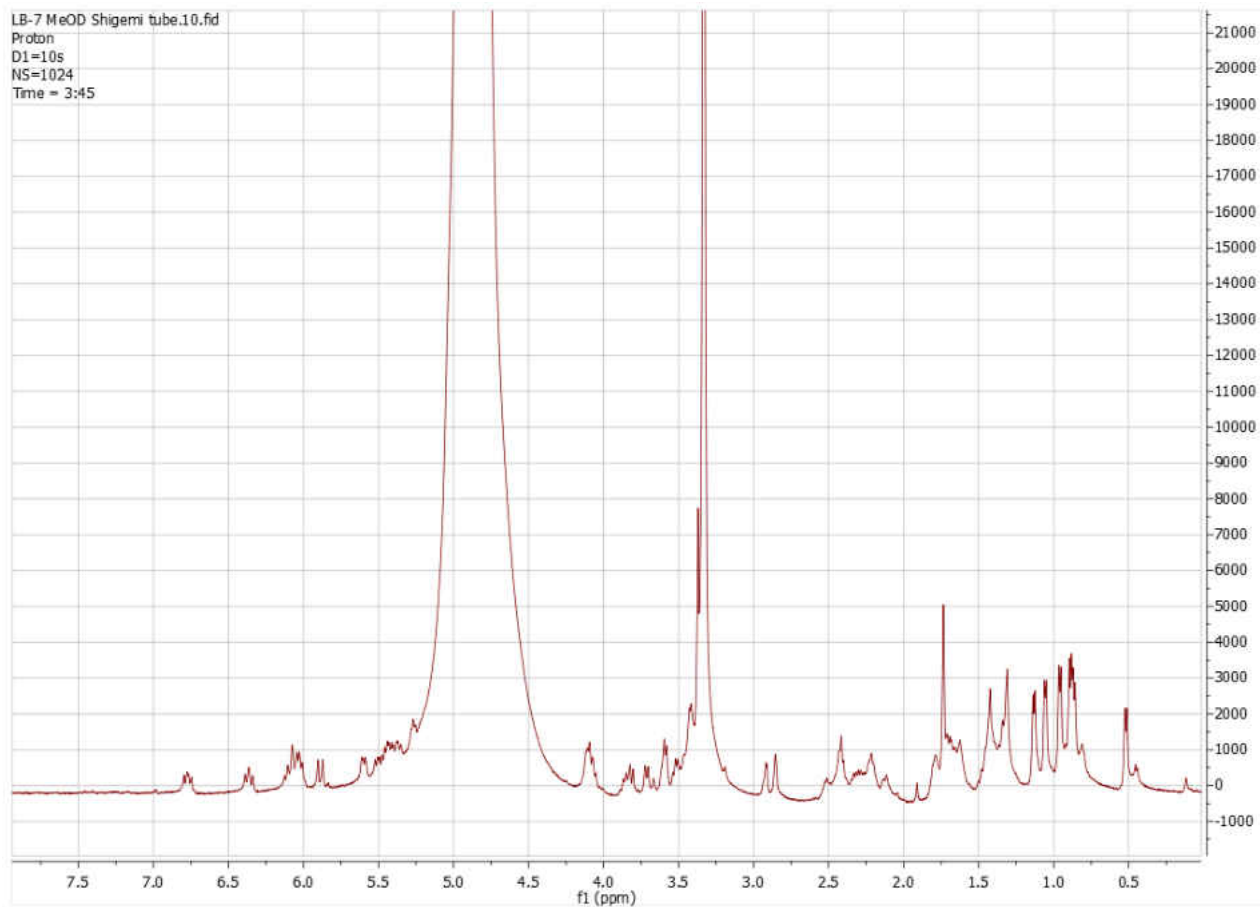
Appendix N: ^{13}C Spectrum of RT.58 Shigemi
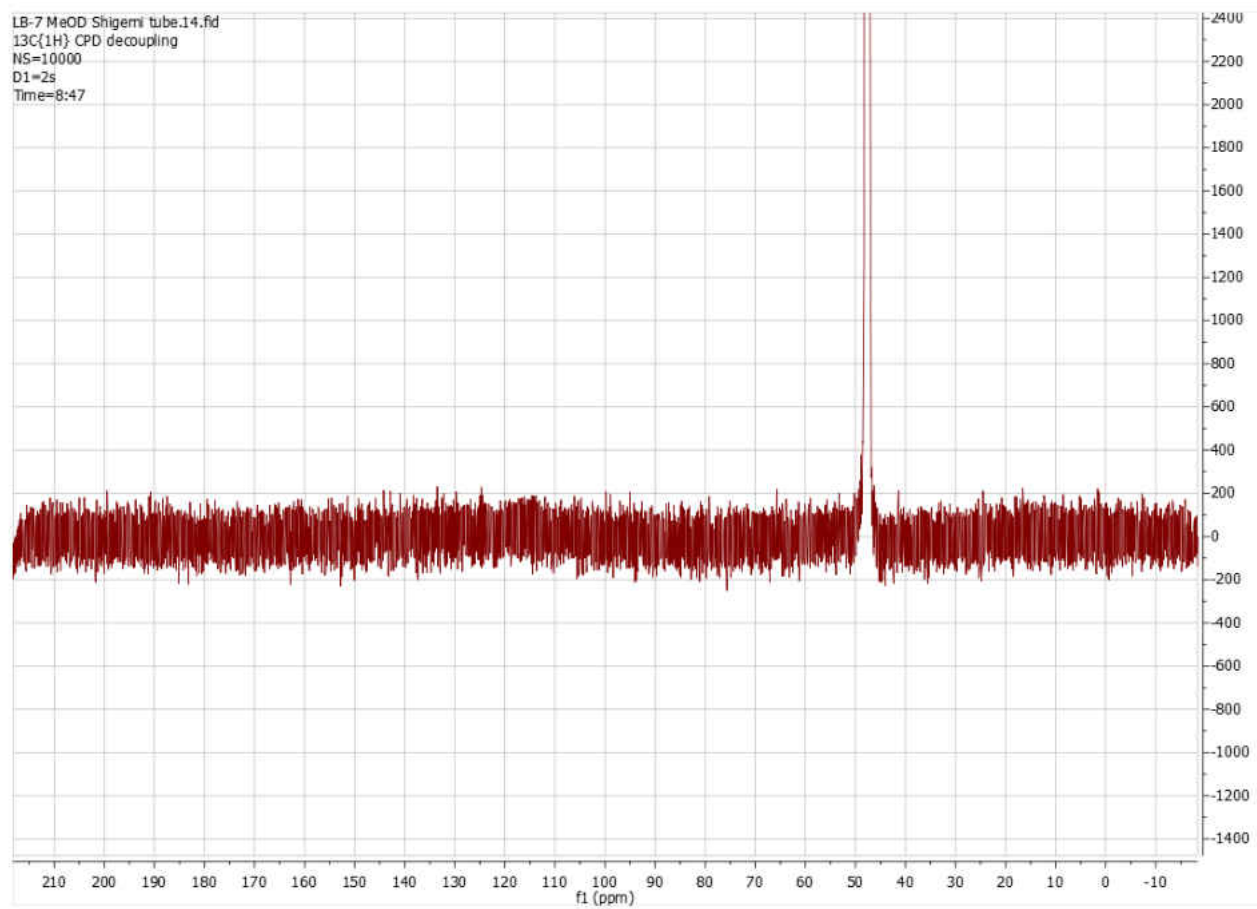
LB-7 MeOD Shigemi tube.14.fid
13C{1H} CPD decoupling
NS=10000
D1=2s
Time=8:47

LB-7 MeOD Shigemi tube.11.ser
COSY
NS=32
TD(F1)=128
Time=1:53

LB-7 MeOD Shigemi tube.12.ser
HSQC_NUS
NUS=50%
NS=64
TD(F1)=256
Time=3:38

LB-7 MeOD Shigemi tube.13.ser
HMBC_NUS
NUS=50%
NS=128
TD(F1)=128

Time=4:16
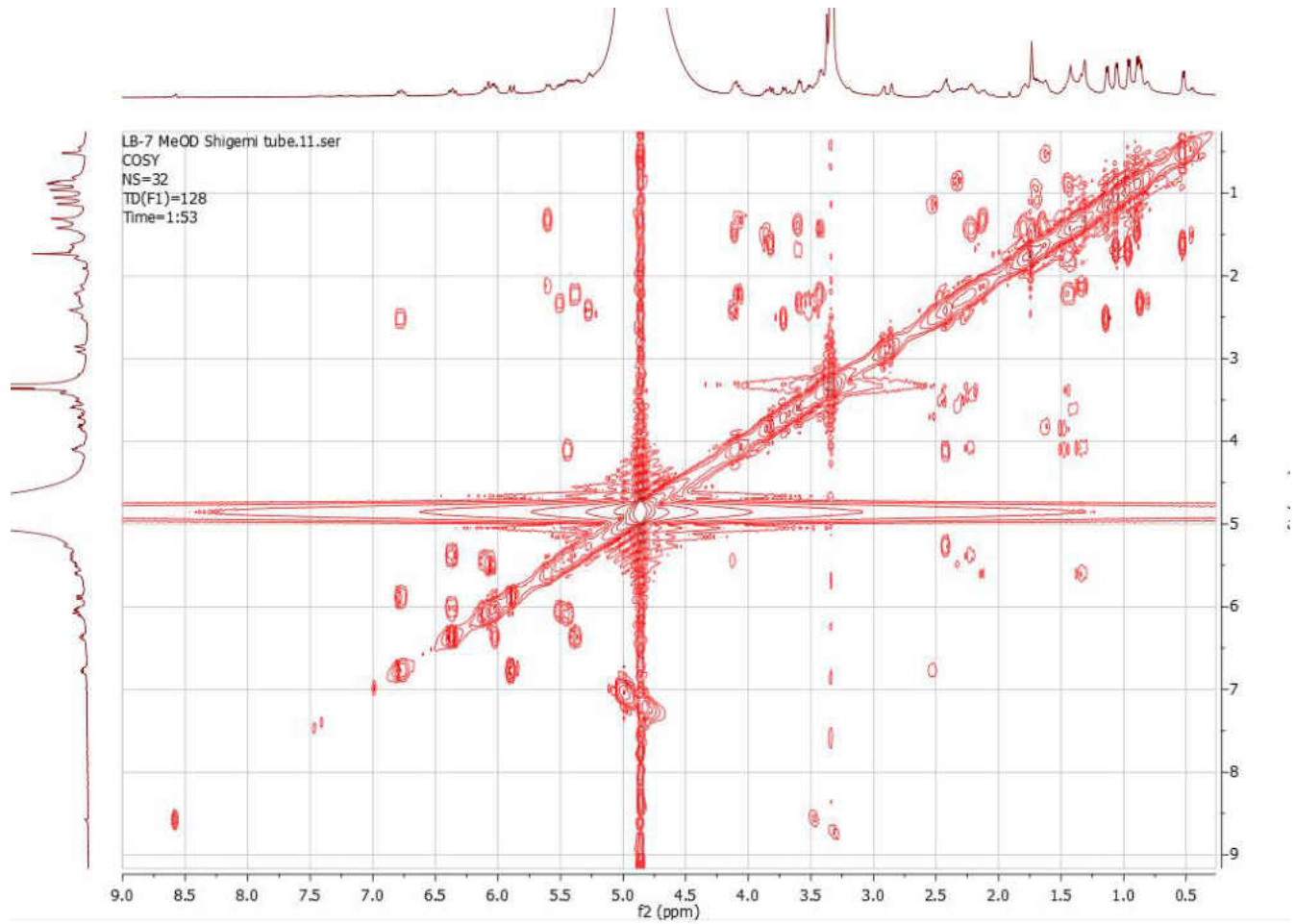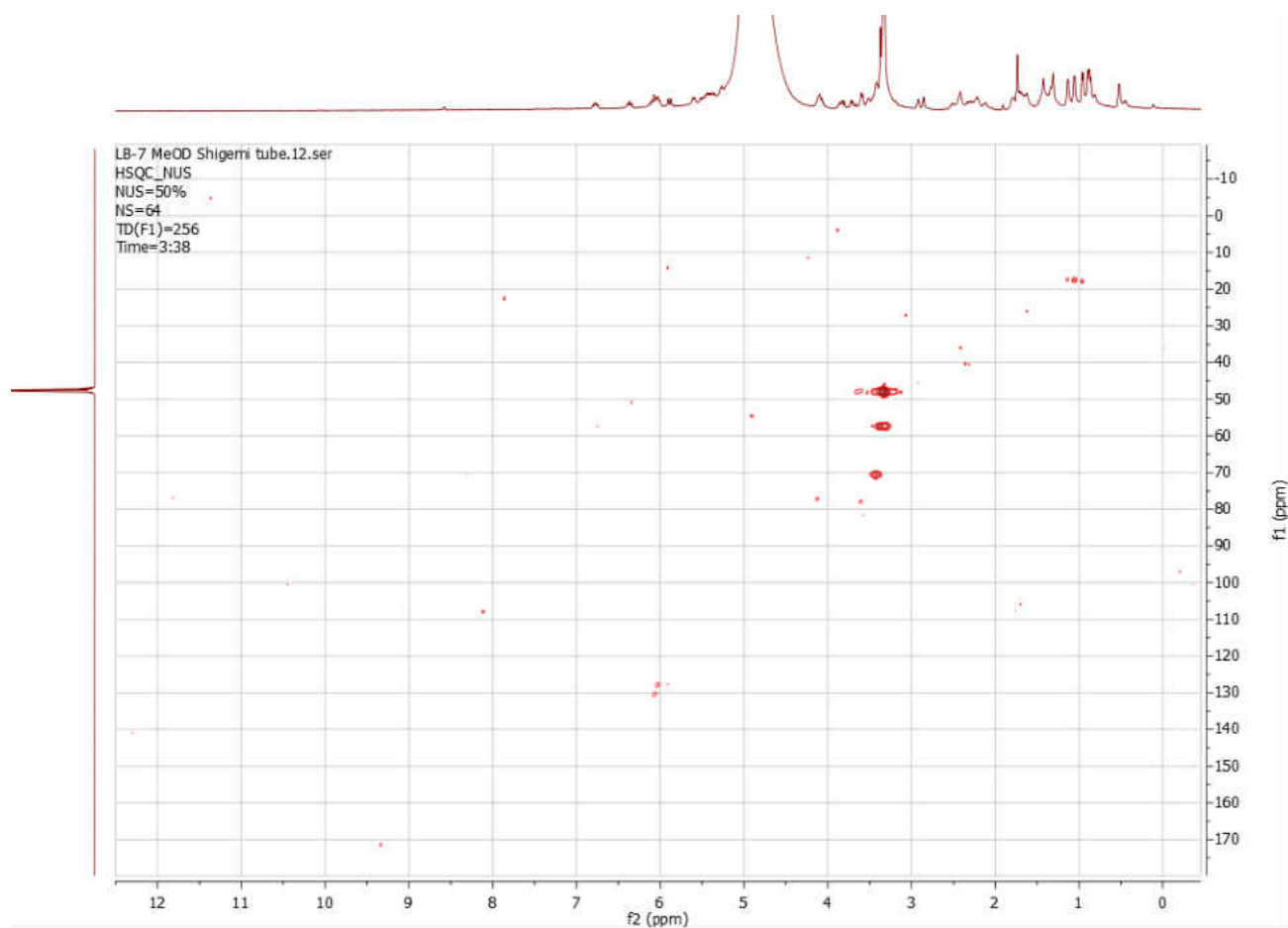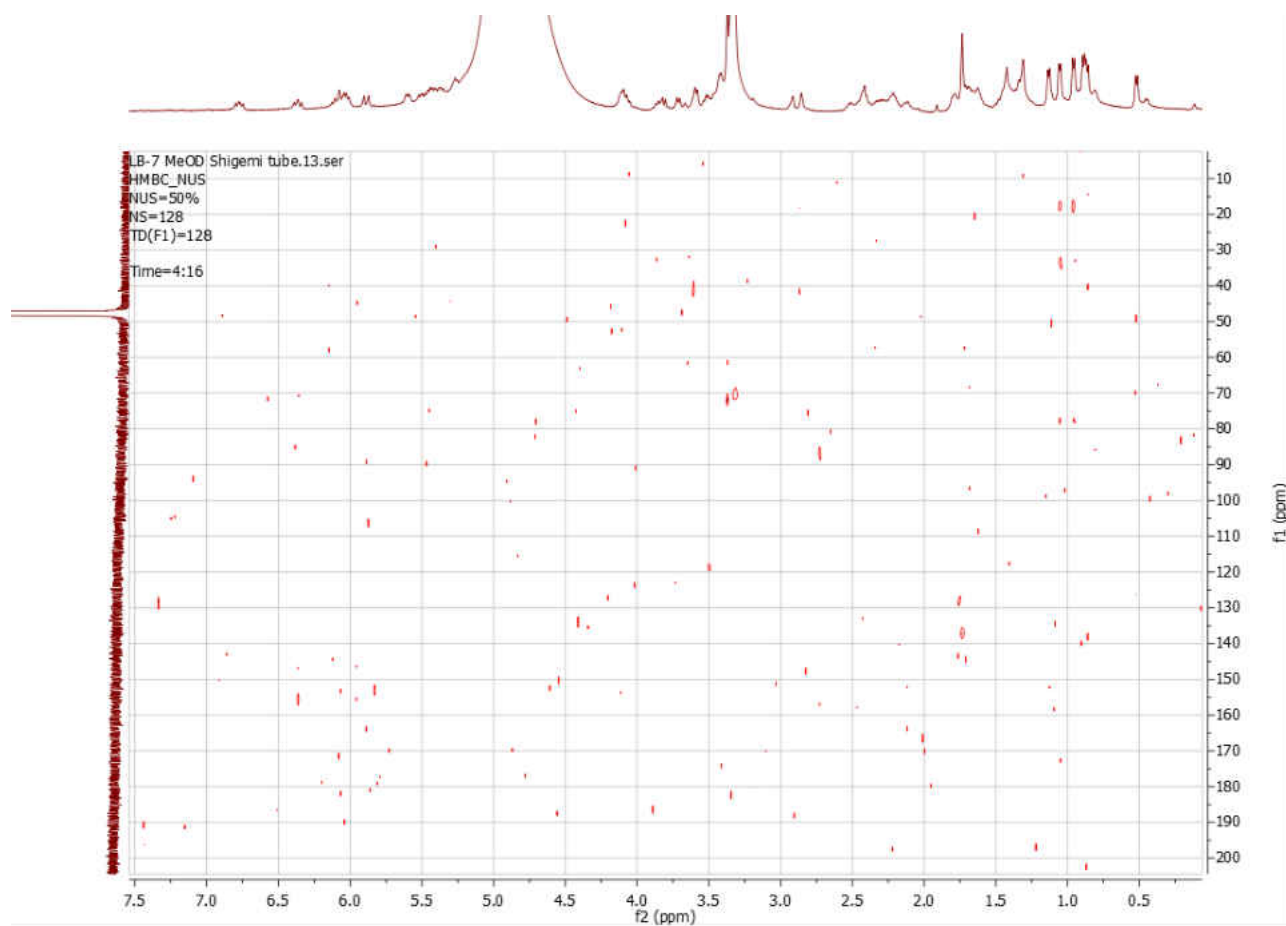
VITA

GARRETT ADAM JOHNSON

Education:	M.S. Chemistry, East Tennessee State University,
	Johnson City, Tennessee, 2019
	B.S. Chemistry, Concord University
	Athens, West Virginia, 2014
Professional Experience	Laboratory Technician, Corporate Innovation
	Eastman Chemical Company, Kinsport, TN, 2014-Present
	Research Assistant, Department of Chemistry
	Concord University, Athens, WV, 2012-2014
Presentations	Garrett Johnson, Pushpa R. Manikindi, Bert C. Lampson
	Abbas G. Shilabin "Partial Structure Assignment of a
	Polyketide Isolated from *Rhodococcus* Bacterium using
	2D-NMR Techniques" 2019 PSNA Annual Conference,
	ETSU, Johnson City, TN, July 21, 2019
	Garrett Johnson, Mohrah Alenazi, Patrick David South, Bert C.
	Lampson, Abbas G. Shilabin "Structure Elucidation of a
	Polyketide Isolated from Rhodococcus MTM3W5.2 via 2-
	D NMR and High-resolution Mass Spectroscopy" South
	East Regional Meeting of the American Chemical Society,
	Charlotte, NC, November 15, 2017